

3-3-81

REPORT NO. NADC-77073-30



NADC  
Tech. Info.

# REAL-TIME X-RAY INSPECTION OF COMPOSITE AIRCRAFT STRUCTURES

F. PATRICELLI, J. BALOGALVIS,  
R. POLICHR and V. J. ORPHAN

December 1978

FINAL REPORT  
AIRTASK No. OTR Rework  
Work Unit No. GA801

*Approved for Public Release; Distribution Unlimited*

8100141

Prepared for  
Naval Air Systems Command  
Department of the Navy  
Washington, D. C. 20360

19970603 022

DTIC QUALITY INSPECTED 3

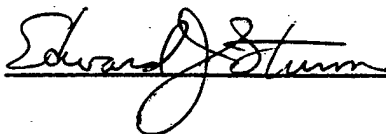
## NOTICES

**REPORT NUMBERING SYSTEM** - The numbering of technical project reports issued by the Naval Air Development Center is arranged for specific identification purposes. Each number consists of the Center acronym, the calendar year in which the number was assigned, the sequence number of the report within the specific calendar year, and the official 2-digit correspondence code of the Command Office or the Functional Directorate responsible for the report. For example: Report No. NADC-78015-20 indicates the fifteenth Center report for the year 1978, and prepared by the Systems Directorate. The numerical codes are as follows:

CODE	OFFICE OR DIRECTORATE
00	Commander, Naval Air Development Center
01	Technical Director, Naval Air Development Center
02	Comptroller
10	Directorate Command Projects
20	Systems Directorate
30	Sensors & Avionics Technology Directorate
40	Communication & Navigation Technology Directorate
50	Software Computer Directorate
60	Aircraft & Crew Systems Technology Directorate
70	Planning Assessment Resources
80	Engineering Support Group

**PRODUCT ENDORSEMENT** - The discussion or instructions concerning commercial products herein do not constitute an endorsement by the Government nor do they convey or imply the license or right to use such products.

APPROVED BY:



DATE:

6/29/79



The major conclusions of the report indicate that RTR can be utilized for composite inspections to detect:

- Porosity
- Bondline voids/discontinuities
- Core damage
- Cracks
- Core splice, plug and filler for repair verification

In addition, the on-site demonstration at the NARF, Norfolk, further illustrated the feasibility of utilizing RTR at the depot level; indicating the inherent advantages which included:

- Ease of set up for inspection
- Immediate presentation for in situ defect analysis
- Electronic video enlargement to improve detectability
- Continuous inspection at varying x-ray energies to highlight either the composite or metallic areas in the structures

These advantages, along with the substantial savings in film costs, will greatly facilitate inspection and extend maintenance capability at all levels.

The second part of the program consisted of developing a penetrant injection system that when coupled with RTR would greatly facilitate assessment of composite damage for delaminations and debonds. A prototype system was fabricated and inspections were performed on graphite/epoxy and boron/epoxy structural samples to determine the feasibility of the technique.

The major conclusions of this part of the report are that, for penetrant injection inspections with 20% aqueous lead acetate solution, RTR will detect:

- 2 mils of solution in a test panel
- The extent of debonds and delaminations in the composite samples

Since the initial feasibility of a penetrant injection system has been demonstrated, SAI is proposing an additional study to develop a portable penetrant injection system that could be used at the 1 and 0 levels for assessment of impact damage for delaminations and debonds. A brief discussion of the proposed program is presented in Section 5.3.

NADC-77073-30

## **AIRCRAFT MAINTENANCE TECHNOLOGY PROGRAM**

**PROGRAM ADMINSTRATOR**

**A. J. KOURY (AIR-4114C)**  
**Naval Air Systems Command**

**PROJECT LEADER**

**D. V. MINUTI (60602)**  
**Naval Air Development Center**

**PROJECT ENGINEER**

**F. PATRICELLI**  
**Science Applications, Inc.**

## FOREWARD

Aircraft composite materials maintenance/repair represents a high priority effort under the Maintenance Technology Program <sup>(1)</sup> and encompasses the applications of effective inspection procedures for all levels of maintenance with a detection of defects in composite structures. Phase I, covering a unique real-time X-ray inspection process, included on-site application for F-14 aircraft at Navaireworkfac-NORVA. Details of Phase I are described in the report and cover capabilities for: (1) detection of material defects, e.g., porosity, bondline voids, discontinuities, cracks, core damage, and (2) repair verification. The major benefit is an immediate visual presentation of hidden flaws. The inspection procedure also eliminates the need for time-consuming handling and processing of X-ray film and is compatible with existing radiographic equipment/capabilities.

---

(1) Sponsored by the Naval Air Systems Command,  
Mr. A. J. Koury (AIR-4114C)

ABSTRACT

Composite aircraft structures were inspected to determine the feasibility of utilizing Real-Time Radiography (RTR) for detection of defects, damage, and repair verification. The program included inspection of composite aircraft structural samples in the laboratory and an on-site demonstration of RTR at the Naval Air Rework Facility (NARF), Norfolk of actual composite aircraft structures.

The major conclusions of the report indicate that RTR can be utilized for composite inspections to detect:

- Porosity
- Bondline voids/discontinuities
- Core damage
- Cracks
- Core splice, plug and filler for repair verification

In addition, the on-site demonstration at the NARF, Norfolk, further illustrated the feasibility of utilizing RTR at the depot level; indicating the inherent advantages which included:

- Ease of set up for inspection
- Immediate presentation for in situ defect analysis
- Electronic video enlargement to improve detectability
- Continuous inspection at varying x-ray energies to highlight either the composite or metallic areas in the structures

These advantages, along with the substantial savings in film costs, will greatly facilitate inspection and extend maintenance capabilities at all levels.

The second part of the program consisted of developing a penetrant injection system that when coupled with RTR would greatly facilitate assessment of composite damage for delaminations and debonds. A prototype system was fabricated and inspections were performed on graphite/epoxy and boron/epoxy structural samples to determine the feasibility of the technique.

The major conclusions of this part of the report are that, for penetrant injection inspections with 20% aqueous lead acetate solution, RTR will detect:

- 2 mils of solution in a test panel
- The extent of debonds and delaminations in the composite samples

Since the initial feasibility of a penetrant injection system has been demonstrated, SAI is proposing an additional study to develop a portable penetrant injection system that could be used at the 1 and 0 levels for assessment of impact damage for delaminations and debonds. A brief discussion of the proposed program is presented in Section 5.3.

### ACKNOWLEDGEMENTS

At this time we would like to thank the various personnel at the NARF, Norfolk (Mr. K. Fizer and Mr. J. Candella) for providing technical assistance, manpower, samples and equipment for the demonstration. In addition, we would like to thank Mr. N. Amdur (NARF, Alameda) and Mr. E. Rosenzweig (NADC, Warminster) for their help in obtaining samples and providing technical assistance on the S-3A. Lastly, we would like to thank Mr. A. J. Koury (AIR-4114C) of the Naval Air Systems Command, Washington, D. C. for his continuing support of RTR development and his help in organizing and coordinating visits to the various Naval activities required during the program.

## TABLE OF CONTENTS

<u>Section</u>	<u>Page</u>
1. INTRODUCTION . . . . .	1
2. BACKGROUND ON COMPOSITE MATERIALS. . . . .	4
3. REAL-TIME IMAGING SYSTEM AND SUPPORTING EQUIPMENT. . . . .	19
3.1 Real-Time Imaging System . . . . .	19
3.2 RTR-100 Sensitivity. . . . .	22
3.3 X-Ray Equipment. . . . .	24
3.4 Photographic Equipment and Documentation . . . . .	24
4. REAL-TIME COMPOSITE INSPECTIONS. . . . .	25
4.1 Direct X-Ray RTR Inspections . . . . .	25
4.2 Penetrant Injection RTR Inspection . . . . .	40
5. SUMMARY, CONCLUSIONS, AND RECOMMENDATIONS. . . . .	54
5.1 Summary of Results . . . . .	54
5.2 Conclusions. . . . .	55
5.3 Recommendations. . . . .	55
REFERENCES . . . . .	57

LIST OF FIGURES

<u>Figure</u>	<u>Page</u>
1. S-3A Graphite/Epoxy Spoiler . . . . .	5
2. F-14 Boron/Epoxy Horizontal Stabilizer. . . . .	6
3. CH--46 Fiberglass Rotor Blade. . . . .	7
4. Composite Damage Classification . . . . .	12
5. Composite Damage Classification . . . . .	13
6. Composite Damage Classification . . . . .	14
7. Example of a Composite Repair . . . . .	16
8. Example of a Composite Repair . . . . .	17
9. SAI Real-Time Radiography System (RTR-100). . . . .	20
10. Diagram of the Interior of the RTR-100 Imaging Unit. . . . .	21
11. RTR of a Fiberglass/Epoxy Helicopter Blade Sample Illustrating Porosity in the Honey- comb (70kV, 5mA) . . . . .	28
12. RTR of a Fiberglass/Epoxy Helicopter Blade Sample Illustrating Bond Line Discontinuities (70kV, 5mA) . . . . .	28
13. RTR of a Graphite/Epoxy Sample with Aluminum Honeycomb Illustrating Damage in a Singular Core (70kV, 5mA). . . . .	29
14. RTR of a Graphite/Epoxy Sample with Aluminum Honeycomb Illustrating Core Damage (70kV, 5mA). . . . .	29

List of Figures (continued)

<u>Figure</u>	<u>Page</u>
15. RTR of a Graphite/Epoxy Sample with Composite Honeycomb Illustrating Moisture Absorption Throughout the Sample (70kV, 5mA) . . . . .	30
16. RTR of a Fiberglass/Epoxy Sample Illustrating Water-Filled Cores in the Honeycomb (70kV, 5mA) . . . . .	30
17. Front Side of a Damaged F-14 Boron/Epoxy Horizontal Stabilizer . . . . .	32
18. Back Side of the F-14 Horizontal Stabilizer . . . . .	32
19. RTR of Area E of F-14 Stabilizer Illustrating the Excessive Honeycomb Damage and Cracks (65kV, 3.5mA) . . . . .	33
20. RTR of Area F of F-14 Stabilizer Illustrating a Large Crack (65kV, 3.5mA) . . . . .	33
21. RTR of Area D Illustrating a Large Area of Crushed Honeycomb in the Right Corner (65kV, 4mA)	34
22. RTR of Area U Illustrating Damage that is Not Visible on the Surface (64kV, 4mA). . . . .	34
23. RTR of Area H Illustrating Where the Honeycomb is Bonded to the Aluminum Honeycomb . . . . .	35
24. RTR of Area H at a Higher X-Ray Energy and Current to Highlight the Metallic Area (95kV, 5mA) . . . . .	35
25. Damaged Fiberglass/Epoxy F-14 Radome Containing a Fiberglass Honeycomb Core . . . . .	37
26. RTR of Area F of the F-14 Radome Illustrating the Cracks and Damaged Honeycomb. . . . .	37

## List of Figures (continued)

<u>Figure</u>	<u>Page</u>
27. Damaged F-14 Radome with an Nick Visible at Area B . . . . .	38
28. RTR of Area B of F-14 Radome Illustrating the Nick (60kV, 3.6mA) . . . . .	38
29. Repaired Area of an S-3A Graphite/Epoxy Spoiler . . . . .	39
30. RTR of Repaired Area Illustrating Splice and Filled Core (70kV, 5mA) . . . . .	39
31. Photograph of Plexiglass Test Panel with Slots of Varying Depths . . . . .	42
32. RTR of Test Panel with a 10% Aqueous Lead Acetate Solution Illustrating the .002, .004, .006, and .008 Inch Depths. . . . .	43
33. RTR of Panel with a 20% Lead Acetate Solution Illustrating a Significant Improvement in Resolving the ,002 Inch Deep Slot . . . . .	43
34. Penetrant Injection System Consisting of Air Pressure/Vacuum Pump, Pressurized Cylinder, and Injector Tip. . . . .	45
35. Photograph of the Injector Tip Before Insertion into the 1/4 Inch Drilled Hole in a F-14 Boron/Epoxy Horizontal Stabilizer Sample. . . . .	46
36. Photograph Illustrating the Operation of the Injection System. . . . .	46
37. Photograph of a Section of a Graphite/Epoxy Sample with Aluminum Honeycomb. . . . .	47
38. RTR of the Damaged Area Illustrating Where the Penetrant has Flowed into the Honeycomb and Possibly between the Laminations Indicating Debonds and Delaminations (65kV, 5mA) . . . . .	48

## List of Figures (continued)

<u>Figure</u>		<u>Page</u>
39.	Electronically Enlarged RTR, Figure 37, Illustrating an Improvement in Detectability . . . . .	48
40.	Photograph of a Small Damaged Area with 1/4 Inch Drilled Hole for the Injector Tip. . . .	49
41.	RTR of the Damaged Section, with no Visible Indication of Damage. . . . .	50
42.	RTR of Damaged Area Illustrating Where the Penetrant has Flowed Throughout the Piece . . . .	50
43.	Photograph of a Six-Ply Graphite Skin with Varying Amounts of Damage . . . . .	52
44.	RTR of Areas Illustrating Where the Liquid has Flowed into the Delaminations (65kV, 5mA) . . .	53
45.	RTR Illustrating Excessive Delaminations Throughout the Area, Indicated by the Large Amount of the Penetrant in the Area (65kV, 5mA). . . . .	53

LIST OF TABLES

<u>Table</u>	<u>Page</u>
1. Common Types of Causes of Composite Damage . . . . .	9
2. NDI Inspection Techniques Utilized for Various Types of Composite Damage. . . . .	10
3. NDI Inspection Techniques Utilized for Various Types of Composite Damage. . . . .	11
4. NDI Techniques Utilized for Composite Repair Verification. . . . .	18
5. SAI RTR-100 Operating Specifications . . . . .	23
6. Composite Samples and Defects Inspected by Direct RTR. . . . .	26

## 1. INTRODUCTION

Science Applications, Inc. (SAI) recently completed a program initiated under the Maintenance Technology Program by Mr. A. J. Koury (Air-4114C) of the Naval Air Systems Command to demonstrate the feasibility of Real-Time Radiography (RTR) for facilitating maintenance inspections at both the intermediate and organizational level. On-site demonstrations were performed at the NARF at Pensacola, North Island and the NAS, Miramar to determine the applicability of RTR for scheduled maintenance, Analytical Rework Program and local engineering specification inspections.

The major results of the program which utilized the SAI RTR-100 portable radiography system were, that for applicable maintenance inspections RTR, had significant advantages over film which included:

- Immediate presentation, examination and interpretation of the inspected part. This was very important in the field inspections of the F-4 and F-5 because the film processing facilities were remote to the inspection location.
- Complex structures containing moving parts could be dynamically inspected to verify proper operation.
- Complex structures containing differing materials and material thicknesses can be continually viewed and inspected by increasing the x-ray energies to highlight the material of interest. In addition, this feature allows the operator to select the optimum x-ray energy and current to produce the most discernible image of the inspected part.

- Small parts can be optically magnified with RTR to enhance the sensitivity and detectability. Electronic parts containing .001 inch broken wires were easily detected with this optical technique coupled with the geometrical magnification made possible by use of a microfocus x-ray generator.
- Costs and time associated with film and film processing would be substantially reduced. The cost savings is approximately \$4.00 per sheet of x-ray film and could be considered to be approximately \$20K per year per maintenance activity.

A report<sup>(1)</sup> was issued in February, 1978 describing the results, conclusions and recommendations of the SAI study.

The successful results of this earlier program in conjunction with some preliminary results on composite samples initiated the present program to determine the feasibility of RTR for inspection of composite airframe structures. The original scope of this program was to perform on-site inspections of composite aircraft structures for material defects that included the following field inspections:

1. S-3A aircraft spoilers at NARF Alameda, California.
2. F-14 horizontal stabilizers at the NARF at North Island, Norfolk and NAS, Miramar.
3. AV-8B aircraft wings at the McDonnell Douglas Corporation, St. Louis, Missouri.

However, because of the limited availability of these composite structures at these locations, the program scope had to be altered. The revised scope of the program was as follows:

1. Perform an on-site inspection of an F-14 horizontal stabilizer at NARF, Norfolk to determine RTR direct imaging sensitivity.
2. Obtain a S-3A spoiler from NAS Alameda to determine the use of RTR for repair verification.
3. Obtain various test composite samples and actual composite structural pieces to determine the sensitivity of RTR for direct viewing of voids, porosity, etc.
4. Develop a prototype system for x-ray opaque penetrant injection to inspect composite structures with RTR for delaminations and debonds.
5. Perform preliminary experiments on the various composite samples to verify the feasibility of utilizing the injection system technique.

Since RTR has previously been demonstrated at various NARF's and was utilized at the NARF, Norfolk in the present program, laboratory experiments on composite structures can be considered to produce results equivalent to those obtainable in the field. In addition, development of the penetrant injection system was oriented toward the design of a field system that could be used at any maintenance level by an experienced radiographer.

This report describes the work demonstrating the feasibility of RTR for composite aircraft structure inspection. A background discussion on composites is presented in Section 2 to acquaint the reader with the technology and Naval utilization. Section 3 of the report describes the Real-Time Radiography System and other equipment utilized in the study. The experimental results for the x-ray RTR inspection of composite structures are presented in Section 4. Section 5 contains a summary of results, conclusions and recommendations.

2. BACKGROUND ON COMPOSITE MATERIALS

Composite materials are becoming more prevalent in the construction of Naval aircraft. Since these materials are fairly new and exhibit properties that differ from conventional aircraft structures, a brief background discussion will be presented to acquaint the reader with the technology and naval utilization, to aid in evaluating RTR as an inspection technique.

Presently, composites are used in varying degrees on Naval aircraft such as the S-3, F-14 and CH-46. These aircraft are unique because they exemplify the use of three types of composites in differing structural applications, as described below and illustrated in Figures 1, 2, and 3.

<u>AIRCRAFT</u>	<u>STRUCTURAL APPLICATION</u>	<u>COMPOSITE TYPE</u>
S-3A	Spoiler (See Fig. 1)	6 ply Graphite/Epoxy skin bonded to an Aluminum Honeycomb
F-14	Horizontal Stabilizer (See Fig. 2)	Boron/Epoxy Skin (8 to 56 plies) bonded to an Aluminum Honeycomb
CH-46	Rotor Blade (See Fig. 3)	2 ply Fiberglass skin bonded to a Nomex Honeycomb

# SPOILER GENERAL DIMENSIONS

NADC-77073-30

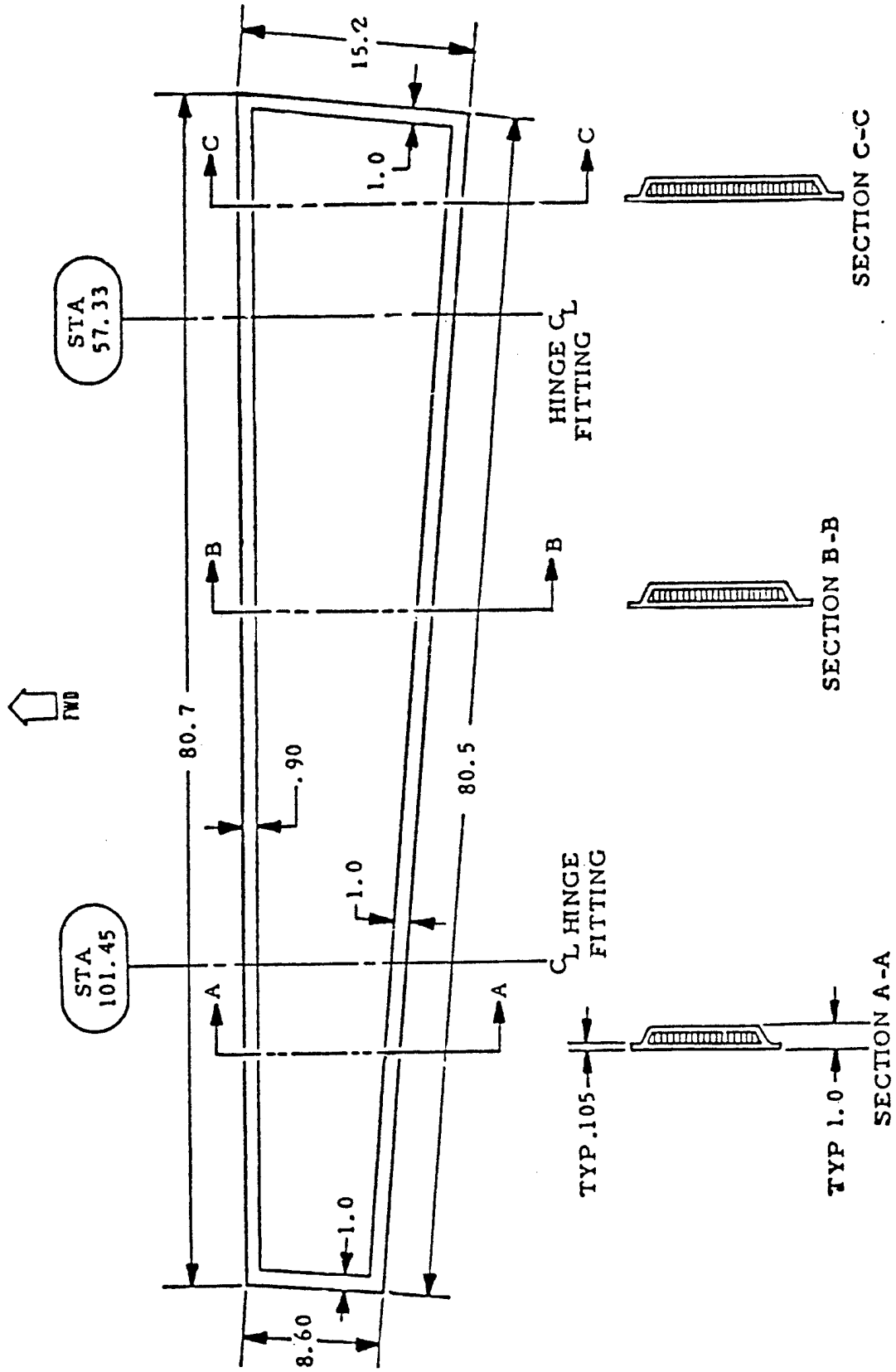


Figure 1. S-3A Graphite/Epoxy Spoiler (2)

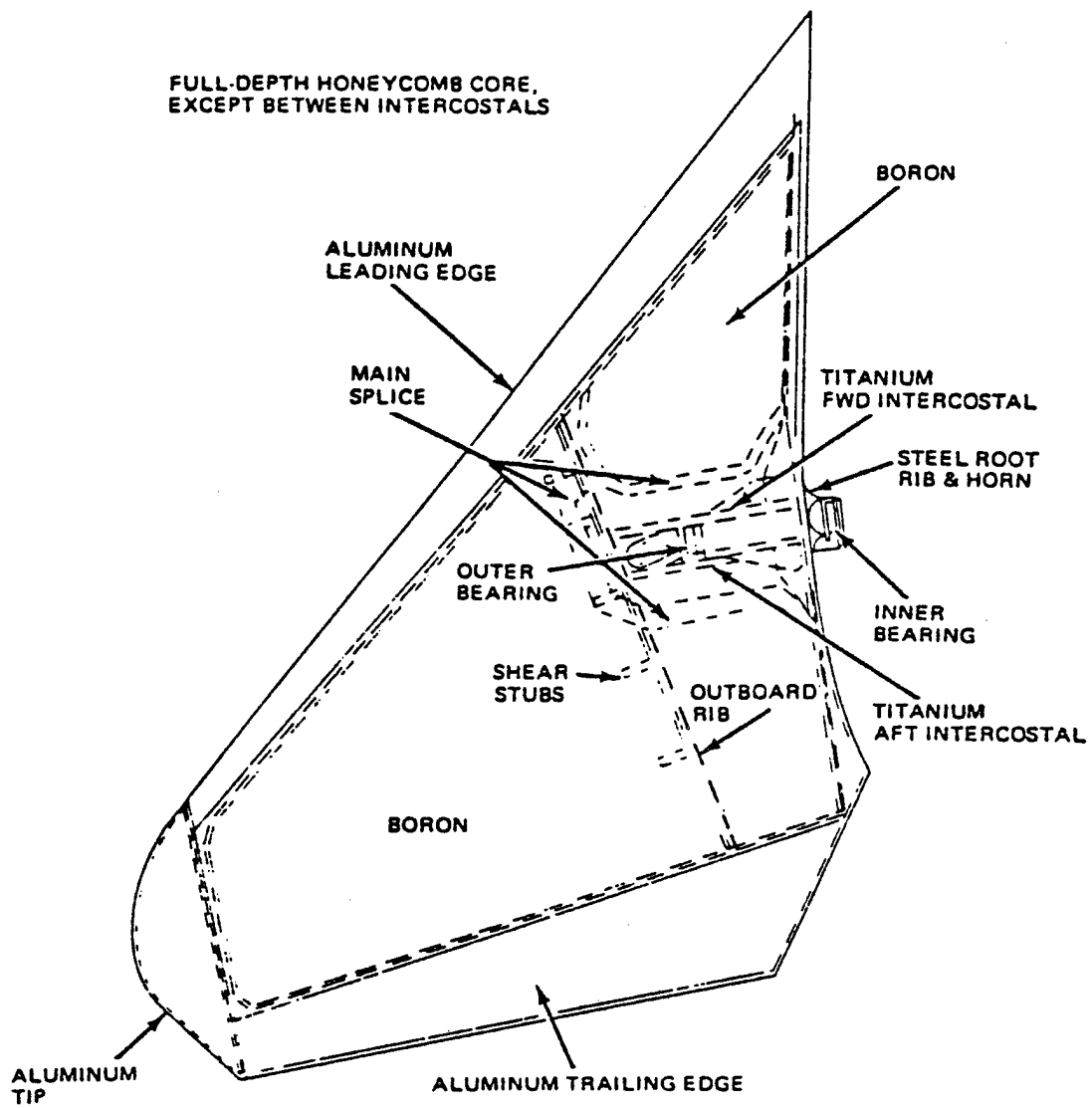
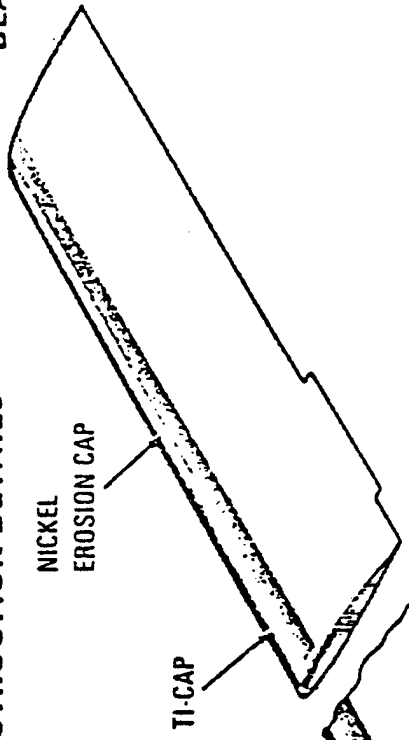
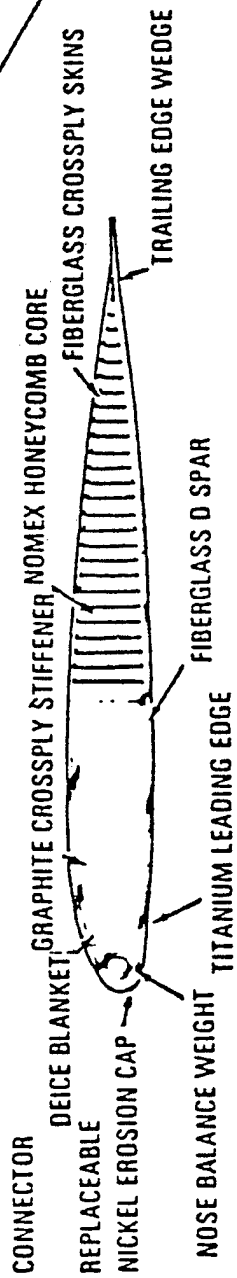
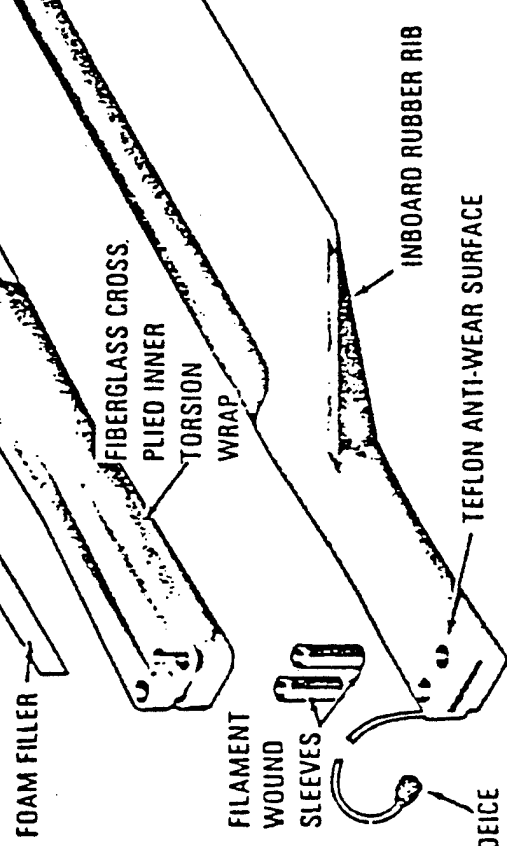


Figure 2. F-14 Boron/Epoxy Horizontal Stabilizer. (3)

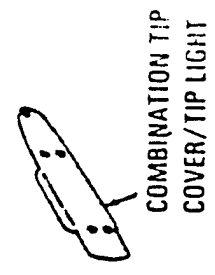
SPAR/ROOT END CONSTRUCTION DETAILS



BLADE PLATFORM



TIP DETAILS



COMBINATION TIP COVER/TIP LIGHT

Figure 3. CH-46 Fiberglass Rotor Blade.

In addition, by the early 1980's, the Navy will have new aircraft such as the F-18, which will consist of graphite/epoxy structural components comprising about 9.5% of their structural weight. Also many aircraft with advanced composite structural designs will be introduced. An example of this design is the AV-8B wing which will be constructed of one piece monolithic graphite/epoxy skins with composite tangent arc spars as substructure.

Although these materials offer superior advantages, such as high strength to weight ratio and corrosion resistant characteristics; they are very susceptible to impact damage that cannot be easily assessed by visual inspection. Table 1 describes the common causes and types of composite damage that can occur in production, environmental exposure and flight line or in-service maintenance of the aircraft. Early detection and assessment of this damage is presently a primary goal of the Navy to insure against structural failure.

Generally, composite aircraft structures are visually inspected and when a suspect area, such as a knick or bubble is encountered, NDI techniques (thru transmission ultrasonics, pulse echo ultrasonics, eddy sonics or x-ray) are utilized to determine the extent of the damage. Tables 2 and 3 describe various NDI techniques presently utilized for inservice and production composite inspection. The next step in the inspection is to classify the damage according to the maintenance specifications relating to the structure. Figures 4, 5 and 6 illustrate typical examples of damage classification used in assessing F-14 horizontal stabilizer damage. After classification, the damage is repaired using specific techniques and materials developed for each individual structure.

Table 1. Common Types and Causes of Composite Damage. (5) (Note 1)

TYPE OF DAMAGE	FLIGHT LINE	PRODUCTION LINE	ENVIRONMENT EXPOSURE
LAMINATE			
<ul style="list-style-type: none"> <li>• DELAMINATIONS</li> <li>• BROKEN FIBERS</li> <li>• DENTS</li> <li>• ABRASIONS</li> <li>• MISDRILLED HOLES</li> <li>• PENETRATION</li> </ul>	<ul style="list-style-type: none"> <li>IMPACTS</li> <li>IMPACTS/CUTS</li> <li>IMPACTS</li> <li>CUTS/SCRATCHES</li> <li>REPAIRS</li> <li>IMPACTS</li> </ul>	<ul style="list-style-type: none"> <li>PROCESSING/IMPACTS</li> <li>PROCESSING/IMPACTS</li> <li>IMPACTS</li> <li>CUTS/SCRATCHES</li> <li>PROCESSING</li> <li>IMPACTS</li> </ul>	<ul style="list-style-type: none"> <li>LIGHTNING/HUMIDITY</li> <li>LIGHTNING</li> <li>LIGHTNING</li> <li>RAIN/SAND EROSION</li> <li>-</li> <li>-</li> </ul>
BONDLINES			
<ul style="list-style-type: none"> <li>• UNBONDS</li> <li>• VOIDS</li> <li>• DEGRADATION</li> </ul>	<ul style="list-style-type: none"> <li>IMPACTS</li> <li>-</li> <li>-</li> </ul>	<ul style="list-style-type: none"> <li>PROCESSING/IMPACTS</li> <li>PROCESSING</li> <li>PROCESSING</li> </ul>	<ul style="list-style-type: none"> <li>LIGHTNING/HUMIDITY</li> <li>-</li> <li>HUMIDITY</li> </ul>
SUBSTRUCTURE			
<ul style="list-style-type: none"> <li>• CRUSHED CORE</li> <li>• BLOWN CORE</li> <li>• CORE NODE UNBOND</li> <li>• CORE CORROSION</li> </ul>	<ul style="list-style-type: none"> <li>IMPACTS</li> <li>-</li> <li>-</li> <li>-</li> </ul>	<ul style="list-style-type: none"> <li>PROCESSING/IMPACTS</li> <li>PROCESSING</li> <li>PROCESSING</li> <li>PROCESSING</li> </ul>	<ul style="list-style-type: none"> <li>LIGHTNING</li> <li>-</li> <li>HUMIDITY</li> <li>HUMIDITY AND SALT</li> </ul>

Note 1 - Data from Naval Air Systems Command, Mr. A. J. Koury (AIR-4114C), Maintenance Technology Program Effort entitled "Non-Destructive Inspection for Damage Assessment of Composite Materials".

Table 2. NDI Inspection Techniques Utilized for Various Types of Composite Damage. (6)  
See Note 1, Page 9.

CONFIGURATIONS CONTAINING LAMINATES  
LAMINATE-LAMINATE BONDS AND/OR LAMINATE-METAL BOND  
TYPE OF CONSTRUCTION

DAMAGE TYPE	BONDED					
	SOLID LAMINATE			LAMINATE TO LAMINATE		
	PRIMARY	BACK-UP	BACK-UP	PRIMARY	BACK-UP	BACK-UP
DELAMINATION	US TT	US PE	US PE	US TT	US PE	US PE
DEBOND	US TT	US PE	US PE	US TT	US PE	US PE
POROSITY	X-RAY US TT	X-RAY US PE	X-RAY US	X-RAY US TT	X-RAY US	X-RAY US TT
VERTICAL BOND VOID	X-RAY	US PE	US PE	X-RAY	US PE	US TT
CRACKS	X-RAY	PENETRANT VISUAL	PENETRANT	X-RAY	PENETRANT	PENETRANT
SPLINTERING	VISUAL	PENETRANT	PENETRANT	VISUAL	PENETRANT	PENETRANT
MOISTURE ABSORPTION	US TT DIELECTRIC	X-RAY	X-RAY	US TT DIELECTRIC	MICROWAVE	MICROWAVE
IMPACT DAMAGE	VISUAL	X-RAY	X-RAY	VISUAL	X-RAY	US PE
BALLISTIC DAMAGE	VISUAL	X-RAY	X-RAY	VISUAL	X-RAY	X-RAY
FIRE OR HEAT DAMAGE	VISUAL	X-RAY US PE	US PE	VISUAL	US PE	EC
RESIN SOFTENING	VISUAL DIELECTRIC	TAP TEST	TAP TEST	VISUAL	TAP TEST	TAP TEST
EROSION	VISUAL	X-RAY	X-RAY	VISUAL	X-RAY	X-RAY

US TT - ULTRASONIC THROUGH TRANSMISSION  
US PE - ULTRASONIC PULSE ECHO  
EC - EDDY CURRENT

Table 3. NDI Inspection Techniques Utilized for Various Types of Composite Damage. (7) See Note 1, Page 9.

CONFIGURATIONS CONTAINING HONEYCOMB CORE

METAL H/C CORE                      NON-METAL H/C CORE

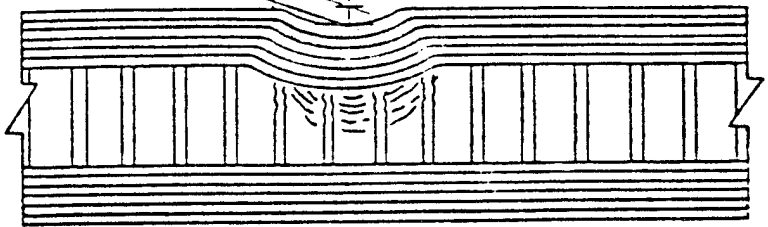
DAMAGE TYPE	<u>METAL H/C CORE</u>		<u>NON-METAL H/C CORE</u>	
	PRIMARY	BACK-UP	PRIMARY	BACK-UP
DELAMINATION FACE SHEET ONLY	EDDY SONIC	USTT	USTT	TAP TEST
DEBOND, FACE TO CORE	USPE	USTT	USPE	USTT
CORE DAMAGE (CRUSHED, NODE SEPARATION, SPLIT)	X-RAY	USTT	X-RAY	USTT
CORE CORROSION	X-RAY	ES	X-RAY	AE
MOISTURE IN CORE	X-RAY	N-RAY	X-RAY	N-RAY
VERTICAL BOND VOID	X-RAY	USPE	X-RAY	X-RAY
IMPACT DAMAGE	VISUAL	X-RAY	VISUAL	X-RAY
FIRE OR HEAT DAMAGE	VISUAL	EC, X-RAY, USPE	VISUAL	X-RAY, US

USTT - ULTRASONIC THROUGH TRANSMISSION  
 USPE - ULTRASONIC PULSE ECHO  
 EC - EDDY CURRENT  
 ES - EDDY SONIC  
 AE - ACOUSTIC EMISSION

NADC-77073-30

0.015-INCH  
MAXIMUM DEPTH

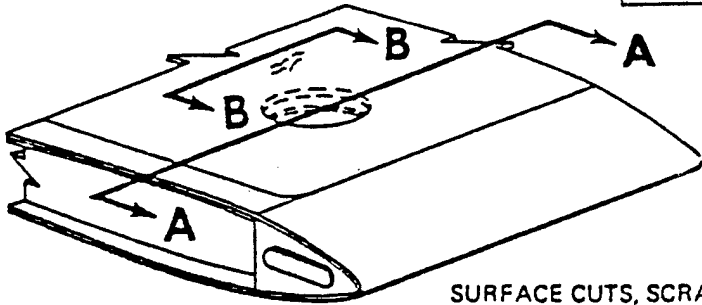
0.500 INCH  
MAXIMUM DIAMETER



SECTION A-A

LIMITS

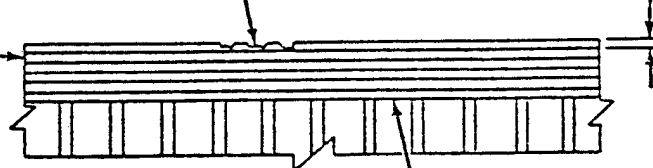
- A. No more than three dents in any 3-inch-diameter circle.
- B. No more than six dents in any 10-inch-diameter circle.



SURFACE CUTS, SCRATCHES AND ABRASIONS  
IN FINAL-FINISH COATING WITH NO DAMAGE  
TO BORON-EPOXY LAMINATE OR ALUMINUM  
LIGHTNING STRIKE STRIPS

ALUMINUM LIGHTNING  
STRIKE STRIP

FINAL-FINISH COATING



BORON-EPOXY LAMINATE

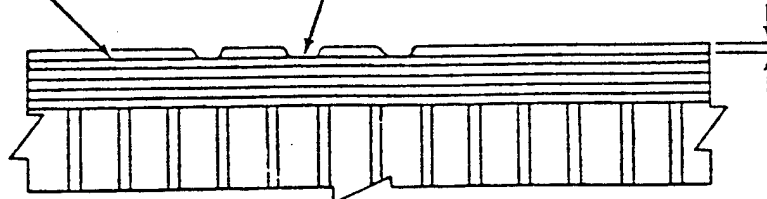
SECTION B-B

CLASS I DAMAGE - NEGLIGIBLE

CUTS, SCRATCHES AND ABRASIONS THAT PENETRATE THE  
ENTIRE FINAL-FINISH COATING, EXPOSING THE BORON-  
EPOXY LAMINATE OR ALUMINUM LIGHTNING STRIKE STRIPS

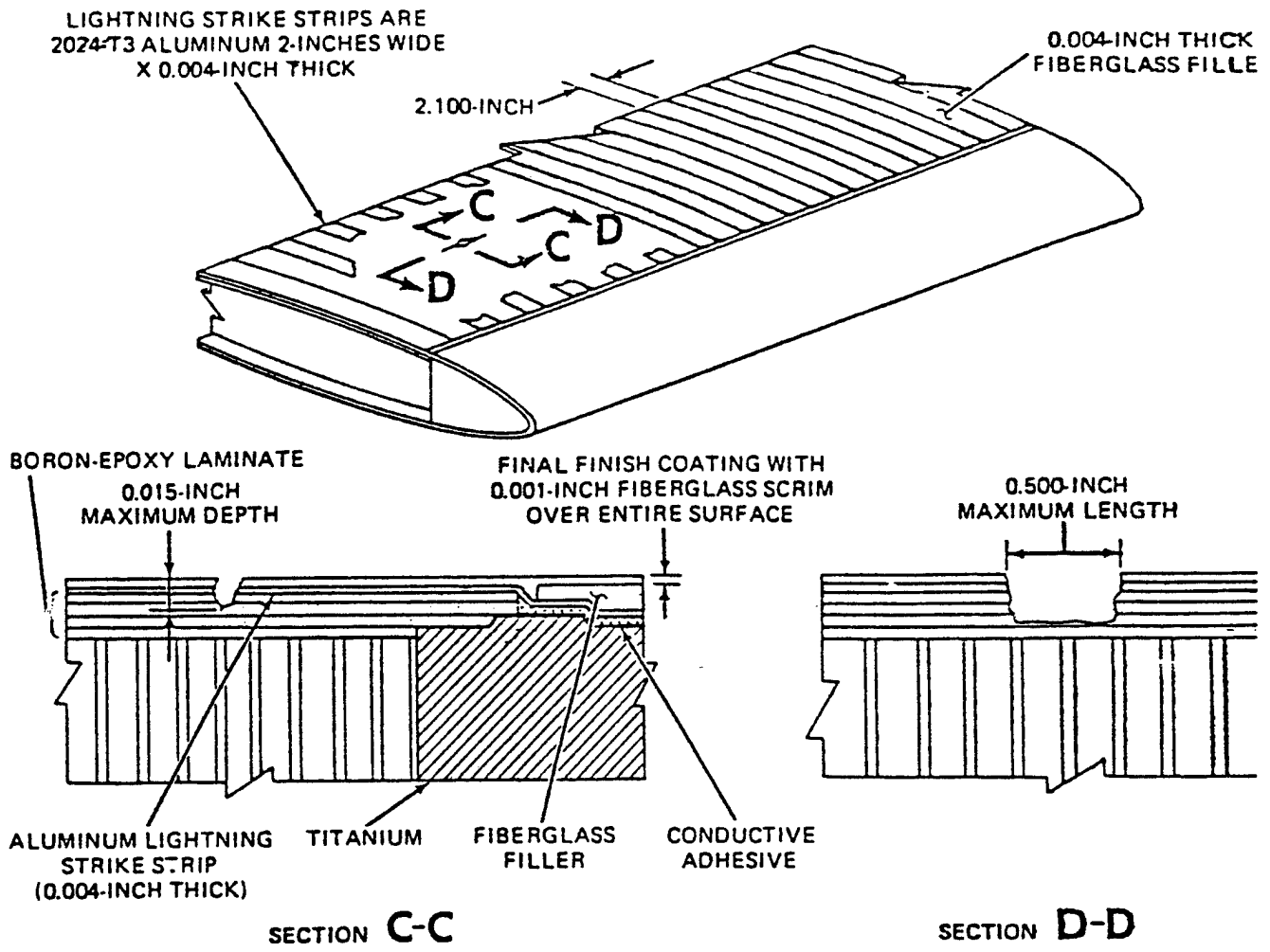
ALUMINUM LIGHTNING  
STRIKE STRIP

FINAL-FINISH COATING

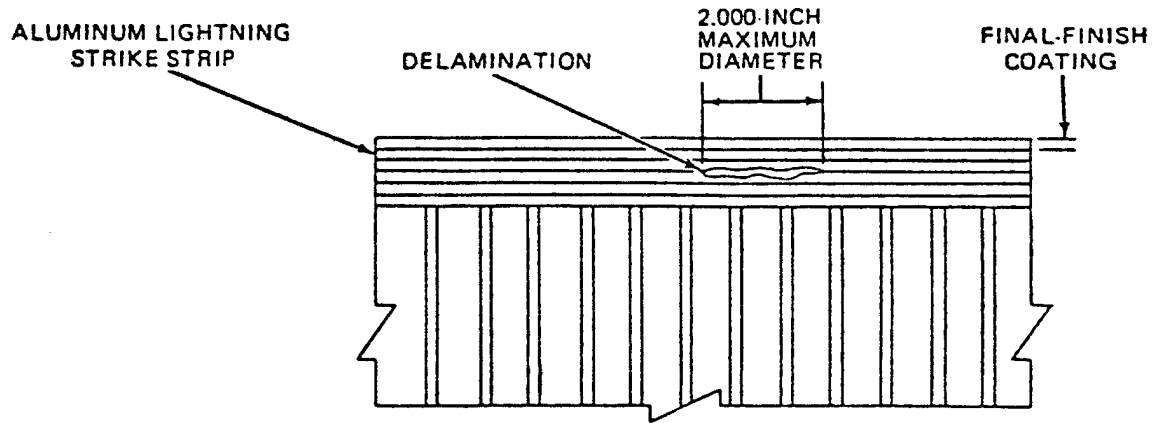


CLASS II DAMAGE - RAIN EROSION

Figure 4. Composite Damage Classification. (8)



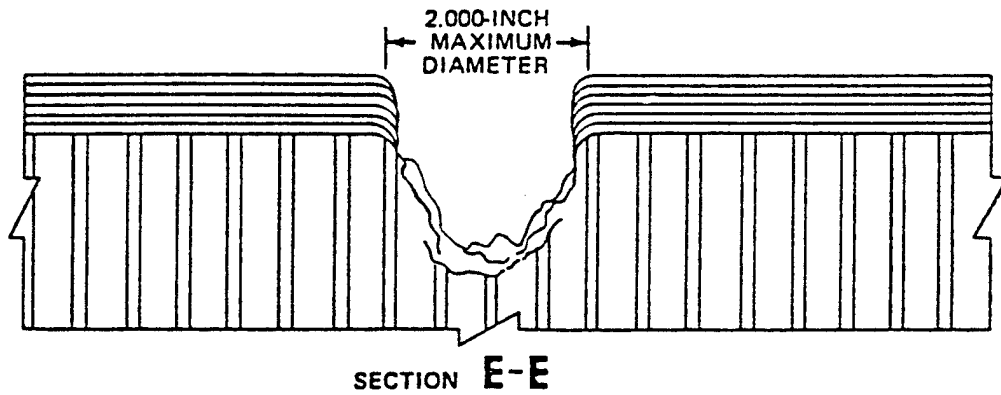
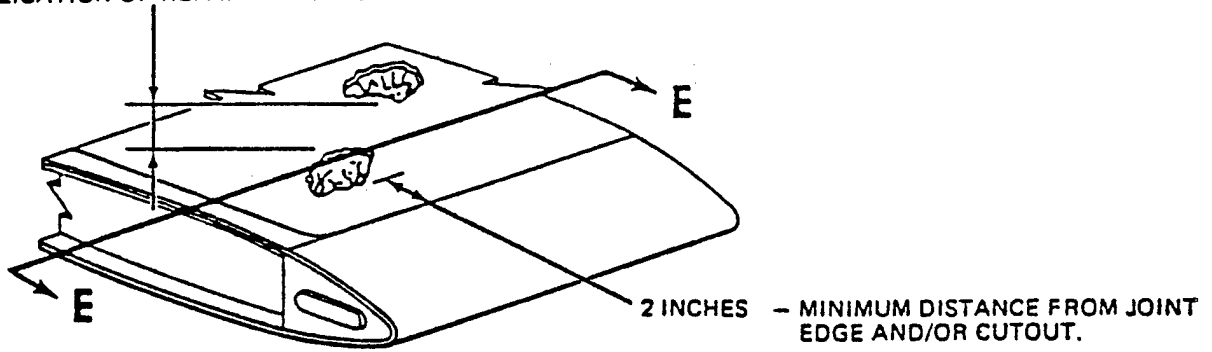
CLASS III DAMAGE - SCRATCHES, CUTS, OR ABRASIONS INTO BORON-EPOXY LAMINATES OR HALFWAY THROUGH LIGHTNING STRIKE STRIPS



CLASS IV DAMAGE - DELAMINATIONS AND VOIDS

Figure 5. Composite Damage Classification. (9)

SPACING BETWEEN REPAIRS SHOULD  
ALLOW SUFFICIENT SPACE FOR  
APPLICATION OF REPAIR PATCHES



CLASS VIII DAMAGE - HOLE DAMAGE RESULTING  
FROM BALLISTIC OR FOREIGN-OBJECT PENETRATION

Figure 6. Composite Damage Classification. (10)

Figures 7 and 8 are illustrative examples of common types of repair utilized for the S-3A spoiler. The final step after repair, is repair verification by an NDI technique as described in Table 4.

In all of these stages of inspection, film x-radiography, as indicated in Tables 2, 3, and 4, is currently used as a routine NDI technique. Therefore, if RTR could be shown feasible for these applications, the inspections and damage assessment would be greatly facilitated.

Presently, for other applications such as assessment of impact damage for debonding and delamination, x-ray techniques are not used, because, generally these types of defects cannot be detected. However, if an x-ray opaque penetrant could be introduced into the suspect area, the extent of the debonds and delaminations could be readily detected with radiography. A newly developed technique which utilizes this concept is discussed in Section 4.2. This technique when coupled with RTR will greatly facilitate the inspections, and in addition, substantially increase inspection capabilities at the I and O level for quick and efficient assessment, and repair of composite structures.

# INJECTION OF ADHESIVE INTO DEBOND

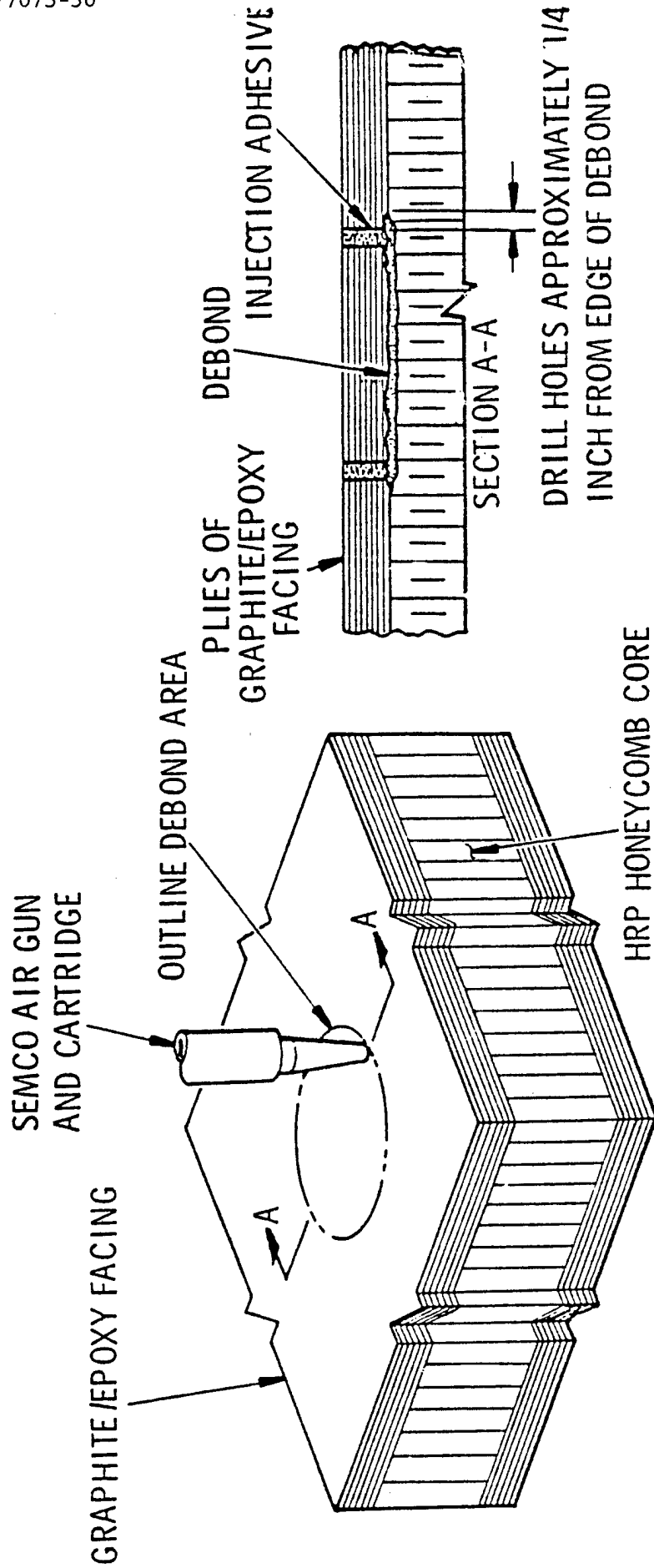


Figure 7. Example of a Composite Repair. (11)

# EXTERNAL PATCH CONFIGURATION

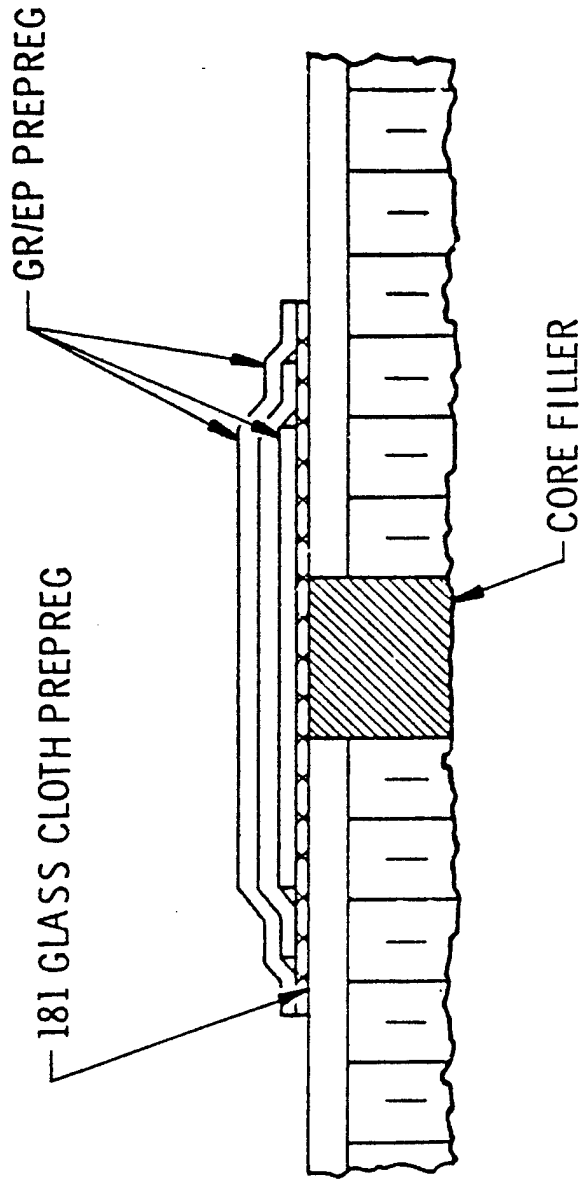


Figure 8. Example of a Composite Repair. (12)

Table 4. NDI Techniques Utilized for Composite Repair Verification. (13)

RESULTS - REPAIR VERIFICATION

TYPE OF REPAIR	PRIMARY	BACK-UP
SURFACE REPAIR	VISUAL	-
LAMINATE REPAIR	USPE	X-RAY, USST
EXTERNAL PATCH - T1/FG	USPE	VISUAL, TAP TEST
EXTERNAL PATCH - G/E	USPE	VISUAL, TAP TEST
EXTERNAL PATCH - B/E	USPE	VISUAL, TAP TEST
EXTERNAL PATCH - BOLTED T1	VISUAL	-
CORE REPAIR - CORE PLUG	X-RAY	USPE, USST
CORE REPAIR - FILLER	X-RAY	USPE, USST
LIGHTNING STRIKE OR STATIC PROTECTION REPAIR	VISUAL	X-RAY

### 3. REAL-TIME IMAGING SYSTEM AND SUPPORTING EQUIPMENT

#### 3.1 REAL-TIME IMAGING SYSTEM

The SAI RTR-100 portable Real-Time Radiography System was used in this program. Figure 9 illustrates the system which consists of the imaging unit, camera control, and videomonitor.

The imaging unit has a 10.5 inch square inspection surface and is fairly portable, weighting only 35 pounds with an overall length of 38 inches. The videomonitor in the figure is the 17" high resolution lab monitor that is rated at 1500 TV lines and has features that include reversible positive/negative and electronic image enlargement. For field applications, a much lighter 7" or 9" monitor can be substituted for the larger lab model. The camera control and monitor can be operated at distances of up to 100 feet from the imaging unit for field inspection. This feature helps protect operating personnel against potential radiation hazards.

Figure 10 illustrates the interior components of the imaging unit that produce the video signal. The system operates by first converting the impinging x-rays at the inspection surface to low level light by a specially designed fluorescent screen. The light is then focused onto the photocathode of a 40mm two stage electrostatic image intensifier with a 35mm f/.95 lens, resulting in a light gain of 2500 and an output resolution of 45 line pairs per mm. The output of the intensifier is fiberoptically coupled to a high resolution vidicon producing a video image on the monitor with 1.5 line pairs per mm resolution. This resolution can be

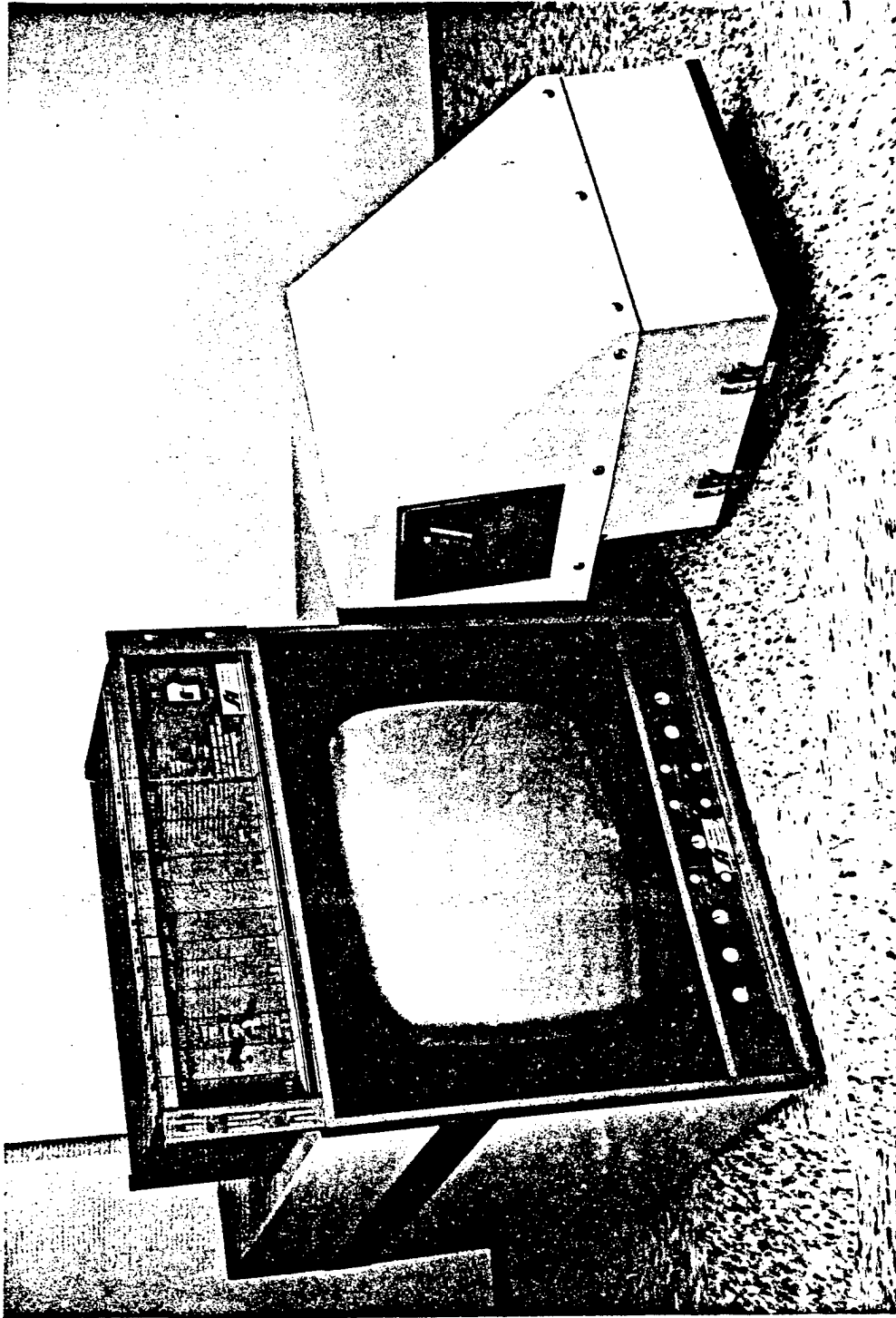
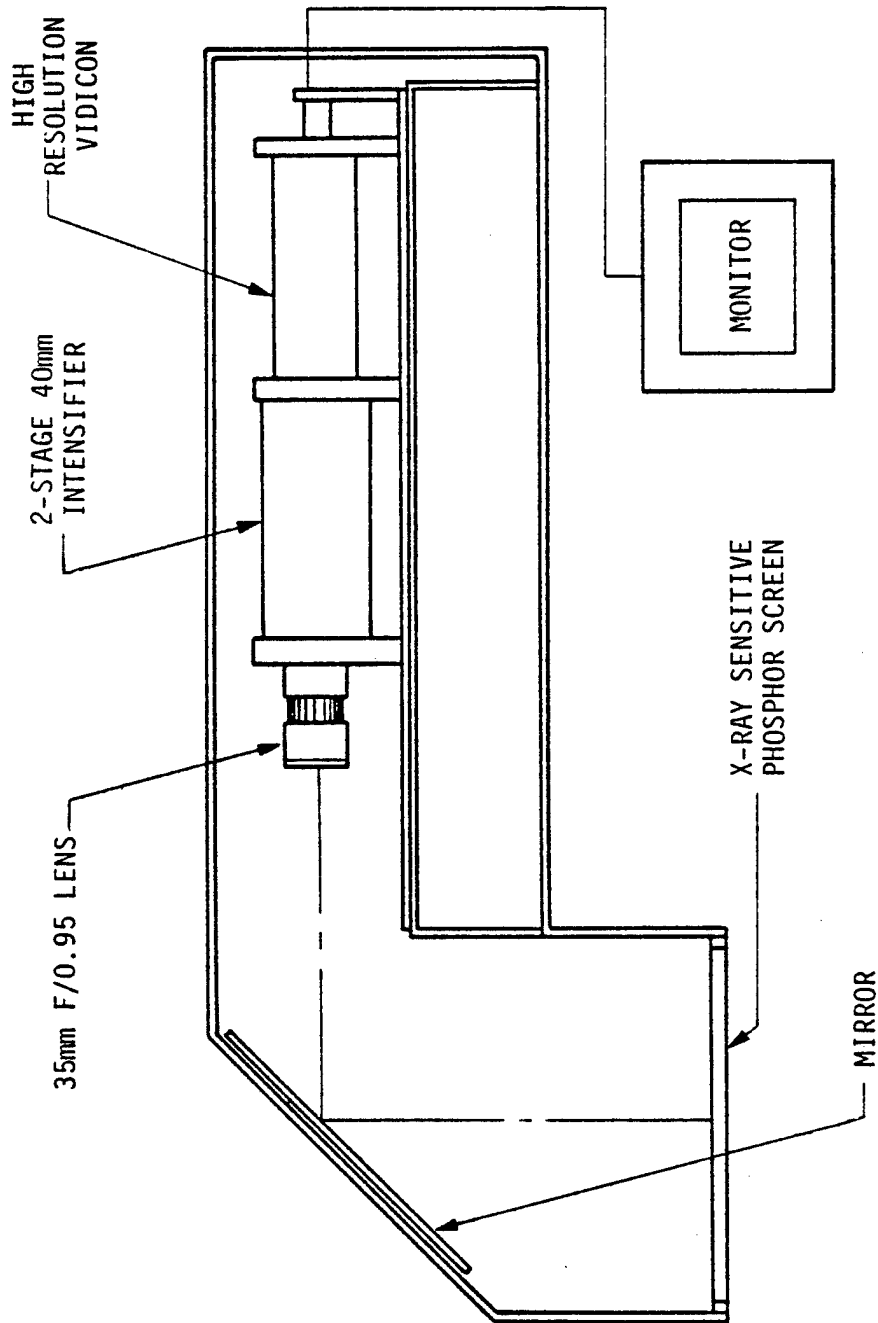


Figure 9. SAI Real-Time Radiography System (RTR-100), Illustrating the Imaging Unit, Camera Control Module, and Videomonitor.



SAI-78FP-30.1

Figure 10. Diagram of the Interior of the RTR-100 Imaging Unit.

easily increased by decreasing the inspection area by a simple lens change. A smaller field size of 6 inches square is commonly used in the RTR-100 which results in a resolution of 2.63 line pairs/mm and an optical magnification of 1.75:1 of the object. For this program both the 10.5 inch and the 6 inch square field sizes were used. The complete operating specifications for the RTR-100 are presented in Table 5.

### 3.2 RTR-100 SENSITIVITY

The sensitivity of the RTR-100 and film will be briefly discussed and compared to illustrate the detection limits of RTR. Since standard penetrameters to measure the radiographic sensitivity aren't readily available, the detection sensitivity of RTR and film will be compared to the results presented in Ref. 1 and 14 and other work performed at SAI.

Presently when film is utilized for maintenance inspections, the limiting resolution, depending on the film type, is between .002 and .003 inch with a contrast sensitivity between 1% and 2% (resolution of 2-T hole on ASTM penetrameter); while for the RTR-100, the limiting resolution is .013 inch for the 10.5 inch square field size and .007 inch for the 6 inch square field size. The contrast sensitivity for the RTR-100 depends mainly on field size, material composition and thickness, varying between 2.5% to 4% (ASTM, 2-T hole).

The discussion illustrates that film is more sensitive than RTR, but as illustrated in the previous report (Ref. 1), there are many applications that don't require this level of sensitivity for adequate detection and assessment of damage. In addition, for applicable inspections, RTR, because of specific inherent advantages, may be superior to film. This report describes applications where RTR is utilized for composite inspections resulting in adequate detection of defects

Table 5. SAI RTR-100 Operating Specifications.

X-ray Phosphor Screen Size	10.5 inches square
X-ray Input Sensitivity	40 kV to 300 kV
Screen Spectral Maximum	550 nm
Video Camera	Vidicon
Scan Rate	30 fps
Signal Bandwidth	18 MHz
Horizontal Resolution	1.64 lp/mm
Vertical Resolution	1.51 lp/mm
Sensitivity (ASTM)	2.5 - 4.0%
Length	38 inches
Depth	12 inches
Height	15 inches
Weight	35 pounds
Power	70 watts, 117 VAC Single Phase 50/60 Hz

and in some cases the results are equivalent or superior to film.

### 3.3 X-RAY EQUIPMENT

Various standard x-ray units were used in the Real Time inspections. Since the inspections were limited to composite structures, only low energy x-rays were necessary for the inspections. At the SAI Laboratory, a portable 160KV Andrex and 160KV Magnaflux X-Ray Unit were utilized. The focal spot of these tubes was 1.5mm. For the NARF, Norfolk inspections, a Sperry 300KV, 10MA and a Baltograph 200KV System were used. The focal spot size of these tubes was approximately 4mm and 2mm respectively.

### 3.4 PHOTOGRAPHIC EQUIPMENT AND DOCUMENTATION

Since the real-time images are viewed on the videomonitor, there are no hard copies as with film. Therefore, in order to document the work, a photographic method was utilized to record the image from the videomonitor. The technique consisted of photographing the monitor with a 4" x 5" Graflex Camera, loaded with Polaroid Type 55 positive/negative film. This allowed immediate development of the images with the resulting negative usable for documentation of the test results. Although the camera and film system offer the best method of documentation, it could not resolve fine detail and low-contrast video images. In addition, it should be noted that the photographic presentation of the video images is not as clear or well-defined as the actual images perceived on the monitor.

#### 4. REAL-TIME COMPOSITE INSPECTIONS

The experimental results of the real-time inspections will now be discussed in two parts. The first section describes direct x-ray imaging for detection of composite defects with the second section discussing a unique penetrant injection technique that will greatly facilitate assessment of impact damage for delaminations and debonds.

##### 4.1 DIRECT X-RAY RTR INSPECTIONS

As previously discussed in Sec. 2, and described in Tables 2, 3 and 4, film x-radiography is routinely used for detection of various types of composite defects. Therefore, if RTR could be utilized for these applications, the times and costs associated with film and film processing would be substantially reduced. In addition, for field and flight line inspections, which are generally remote to film processing facilities, the inspection including defect analysis could be completely performed at the inspection site. This would greatly reduce maintenance inspection times, thus reducing the amount of down time of strategic aircraft. This section describes the utilization of RTR for inspection of composites for these types of defects to illustrate the feasibility of RTR as a complementary/replacement technique for film.

Table 6 lists the composite samples and defect types that were inspected by direct RTR. Some of the composite structures are laboratory samples that were inspected at SAI, while other samples were actual structural pieces that were inspected at the NARF, Norfolk and SAI. The results will now be presented

Table 6. Composite Samples and Defects Inspected by Direct RTR.

COMPOSITE DEFECT	COMPOSITE SAMPLES
Porosity	<ul style="list-style-type: none"> <li>● Fiberglass/Epoxy Helicopter Blade lab sample</li> <li>● F-14 Fiberglass/Epoxy Radome</li> </ul>
Bond Voids/ Discontinuities	<ul style="list-style-type: none"> <li>● Fiberglass/Epoxy Helicopter Blade lab sample</li> <li>● F-14 Boron/Epoxy Horizontal Stabilizer</li> </ul>
Cracks	<ul style="list-style-type: none"> <li>● F-14 Boron/Epoxy Horizontal Stabilizer</li> </ul>
Moisture Absorption	<ul style="list-style-type: none"> <li>● Graphite/Epoxy lab samples with Fiberglass Honeycomb</li> <li>● Fiberglass/Epoxy Helicopter Blade lab sample</li> </ul>
Core Damage	<ul style="list-style-type: none"> <li>● Graphite/Epoxy lab samples with Aluminum Honeycomb</li> <li>● F-14 Boron/Epoxy Horizontal Stabilizer</li> <li>● F-14 Fiberglass/Epoxy Radome</li> </ul>
Core Plug/Filler Repair Verification	<ul style="list-style-type: none"> <li>● S-3A Graphite/Epoxy Spoiler</li> </ul>

and discussed for these inspections, with the x-ray energies and current utilized for each application printed in parenthesis with the appropriate figure.

The first type of defect listed in Table 6, porosity and bond voids/discontinuities, are generally manufacturing defects, but in some cases they can result from erosion. Fig. 11 is an RTR (Real-Time Radiograph) of a fiberglass/epoxy helicopter blade sample illustrating porosity in the honeycomb (light and dark areas). The next RTR, Fig. 12, of the same sample shows adhesive discontinuities on the bond line of the blade. These radiographs illustrate the sensitivity of real-time radiography to easily detect non-uniformities occurring in the composite structure.

Another common type of composite defect listed on Table 6 is core damage. This can either occur during manufacturing or result from impact or ballistic damage. Figure 13 shows an RTR of a graphite/epoxy sample with a single damaged cell resulting from manufacturing. Another example, Fig. 14, is an RTR of a graphite/epoxy sample with the honeycomb core damaged by impact. These examples illustrate the sensitivity of RTR for detection of core damage even as minute as damage to a single cell.

Moisture absorption is a type of damage that results from continuous environmental exposure of the composite structure. This type of damage usually produces erosion, which can subsequently result in failure. Figure 15 is an RTR of a graphite/epoxy sample that contains varying amounts of moisture throughout the piece. The next RTR, Fig. 16, shows where water has collected in the honeycomb cells of a fiberglass/epoxy sample. Moisture absorption is a common problem with aircraft deployed on carriers, which could be easily inspected with RTR for quick detection and immediate assessment.

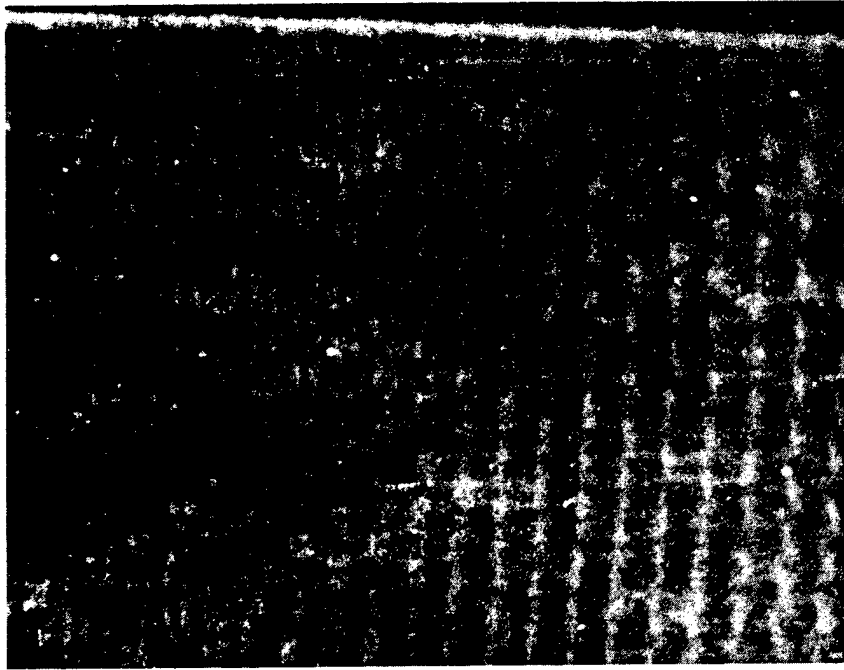


Figure 11. RTR of a Fiberglass/Epoxy helicopter blade sample illustrating porosity in the honeycomb. The light areas indicate adhesive rich areas, with the dark areas indicating lack of adhesive (70kV, 5mA)

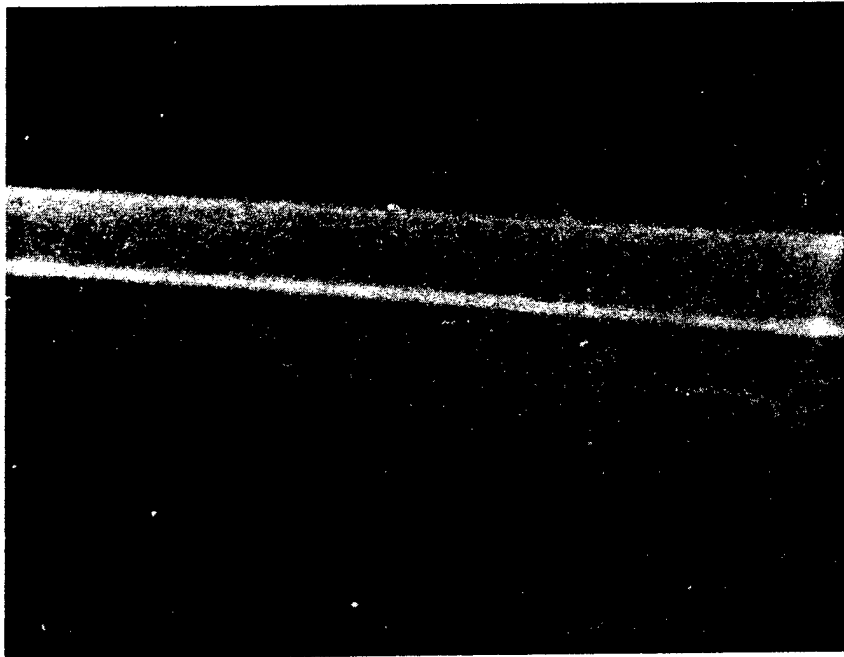


Figure 12. RTR of a Fiberglass/Epoxy helicopter blade sample illustrating bond line discontinuities (70kV, 5mA)

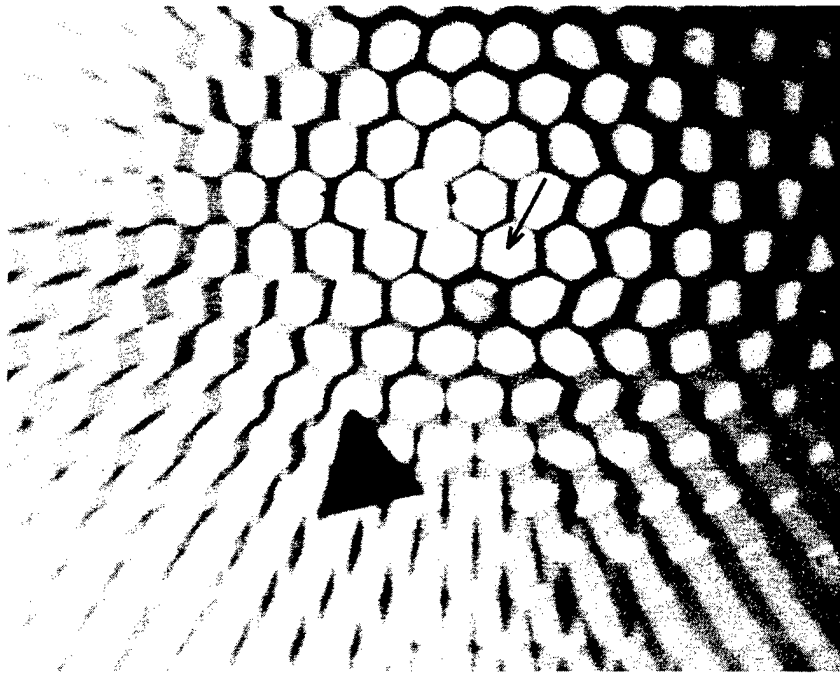


Figure 13. RTR of a Graphite/Epoxy sample with aluminum honeycomb illustrating damage in a singular core (70kV, 5mA)

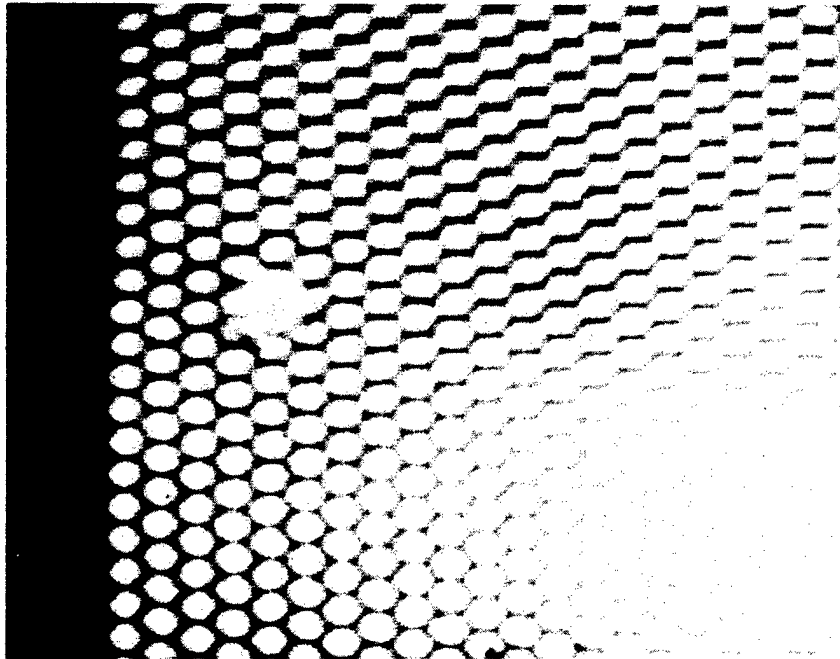


Figure 14. RTR of a Graphite/Epoxy Sample with Aluminum Honeycomb illustrating core damage (70kV, 5mA)

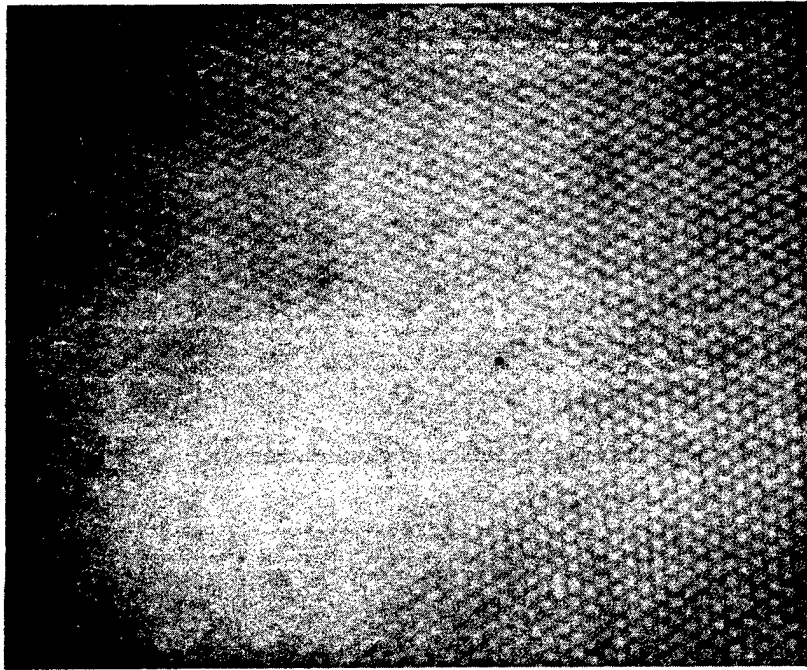


Figure 15. RTR of a Graphite/Epoxy sample with composite honeycomb illustrating moisture absorption throughout the sample (70kV, 5mA)

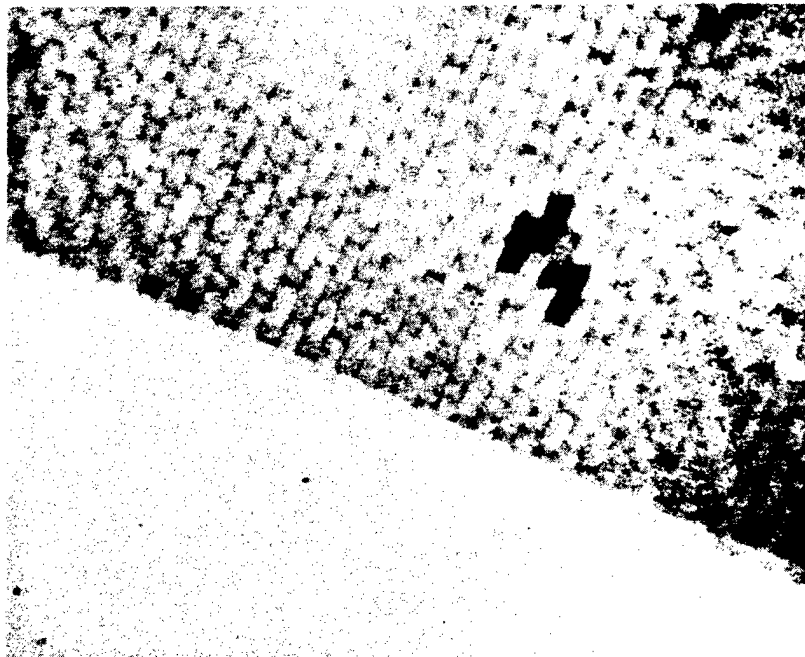


Figure 16. RTR of a Fiberglass/Epoxy sample illustrating water-filled cores in the honeycomb (70kV, 5mA)

In order to demonstrate the feasibility of RTR for inspection of actual composite structures, an on-site demonstration was performed at the NARF, Norfolk. Two damaged composite aircraft structures, a F-14 horizontal stabilizer and a F-14 radome, were selected for the demonstration. The horizontal stabilizer was boron/epoxy with aluminum honeycomb, while the radome consisted of fiberglass/epoxy with a fiberglass honeycomb.

Figures 17 and 18 show the front (x-ray source side) and back (next to RTR screen) of a damaged F-14 stabilizer labelled with lead letters at different areas to identify the area during inspection. The photographs illustrate extensive damage at D, E and F, with no visible damage at C, H and U. Areas B and G contain small nicks that are visible on the surface.

Figures 19, 20 and 21 are the RTR's of areas D, E and F illustrating the extensive skin and honeycomb damage. Figures 19 and 20 of areas E and F indicate extensive core damage and various cracks (light areas). In addition, area D, Fig. 21, illustrates single cell damage similar to the damaged cell produced during manufacturing (Fig. 13). Area U is shown in Fig. 22, with varying amounts of damage indicated in the upper right quadrant. Areas B and G that contained the nicks were inspected, with the small nick at B barely visible on the videomonitor. Although the nick at area G could be seen on the monitor, it was impossible to photograph. The last area, H, was radiographed to show where the composite and metal are bonded. Figure 23, of the area shows the variations in the adhesive bonding the honeycomb structure to the aluminum. Figure 24, another RTR of area H, is a radiograph taken with increased x-ray energy and current to image the metallic area which is not very visible

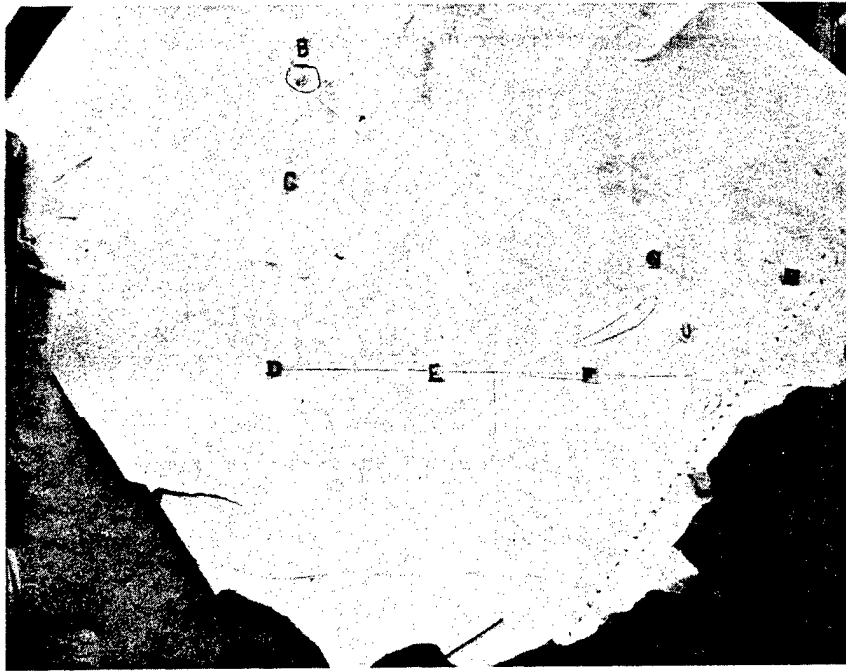


Figure 17. Front Side of a damaged F-14 Boron/Epoxy horizontal stabilizer

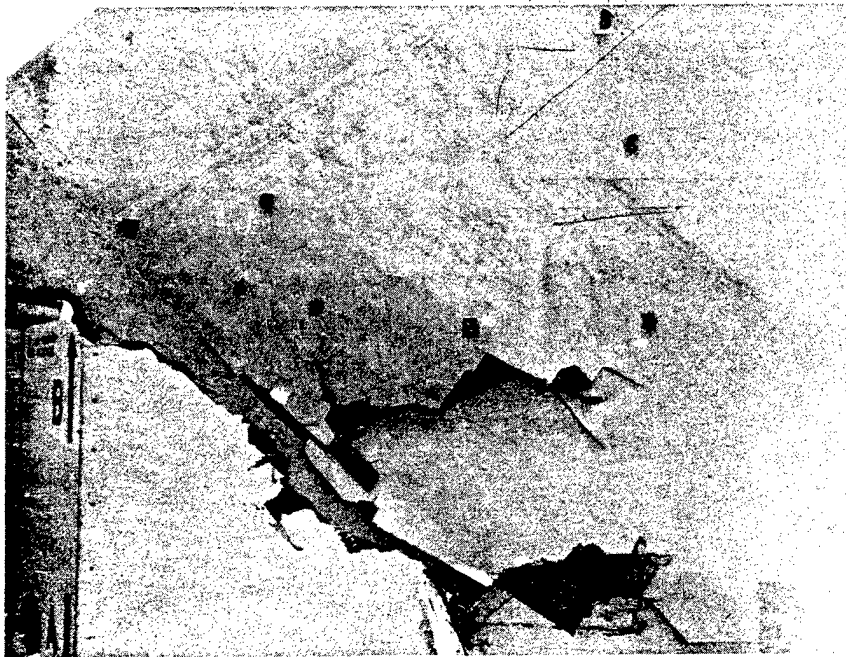


Figure 18. Back side of the F-14 horizontal stabilizer

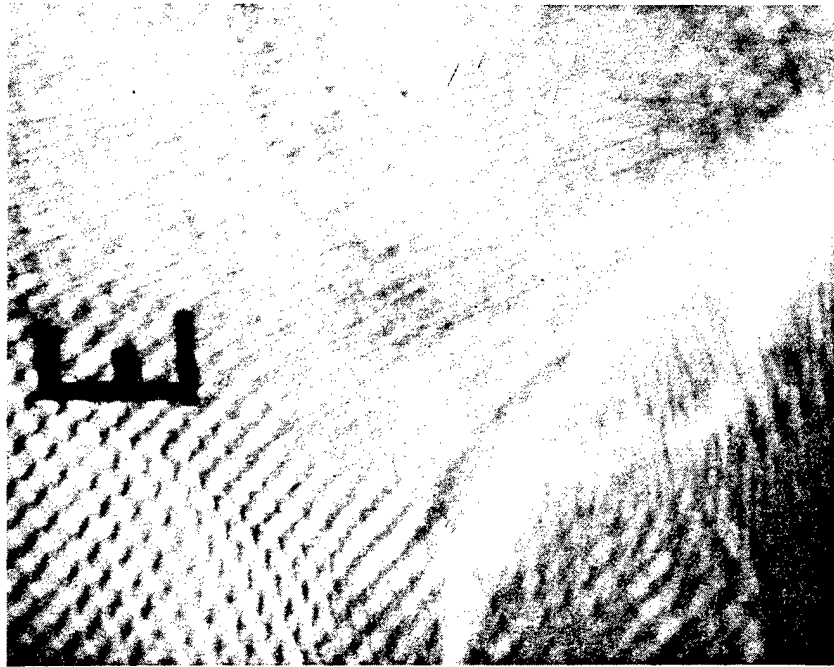


Figure 19. RTR of area E of F-14 stabilizer illustrating the excessive honeycomb damage and cracks (65kV, 3.5mA)

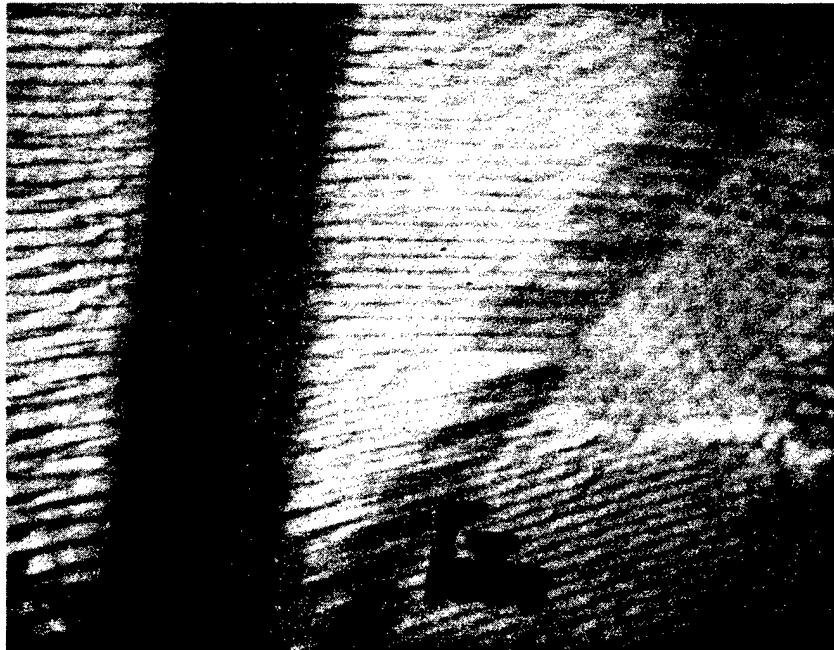


Figure 20. RTR of area F of F-14 stabilizer illustrating a large crack (indicated by the light area) (65kV, 3.5mA)

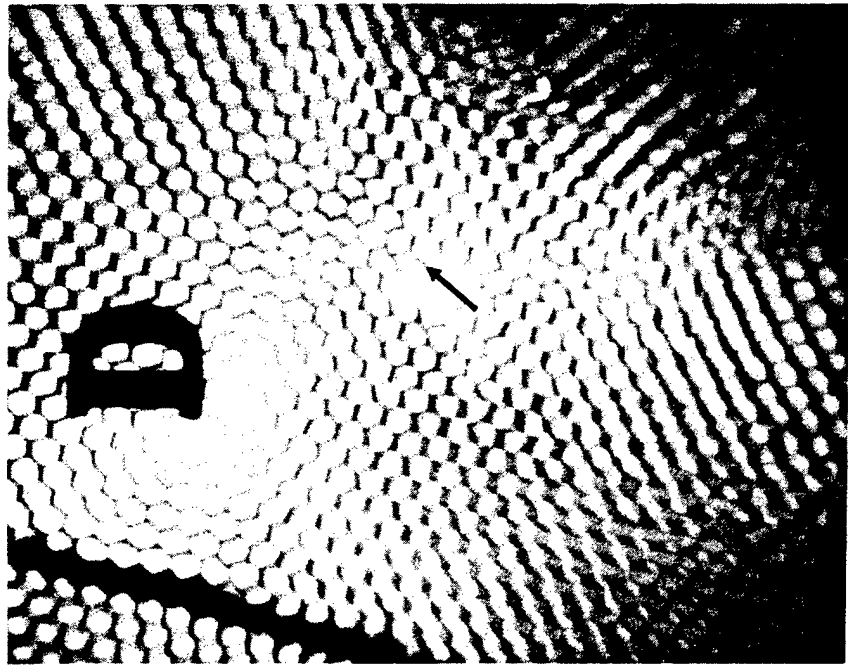


Figure 21. RTR of area D illustrating a large area of crushed honeycomb in the right corner. In addition a singular core indicates core damage similar to the type in Figure 13. (65kV, 4mA)

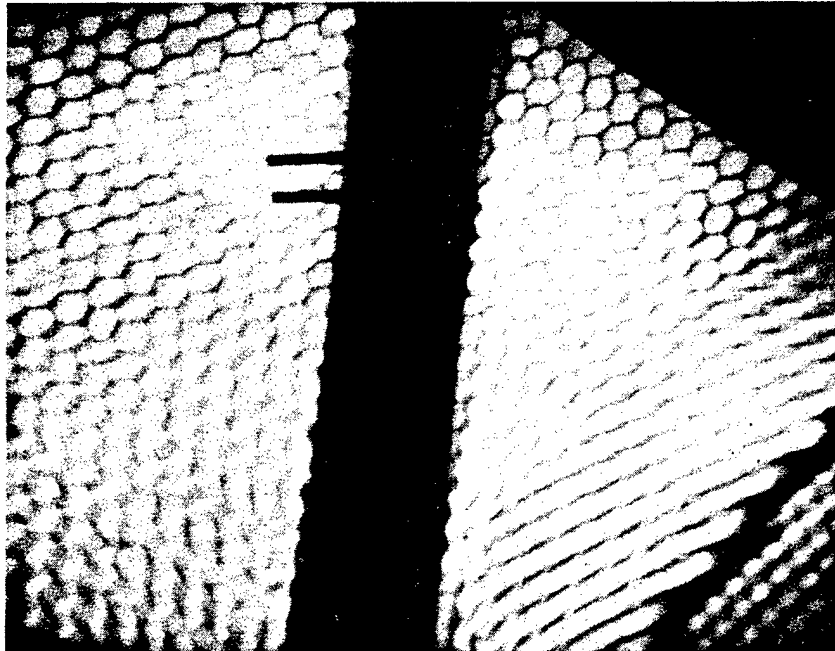


Figure 22. RTR of area U illustrating damage that is not visible on the surface (64kV, 4mA)

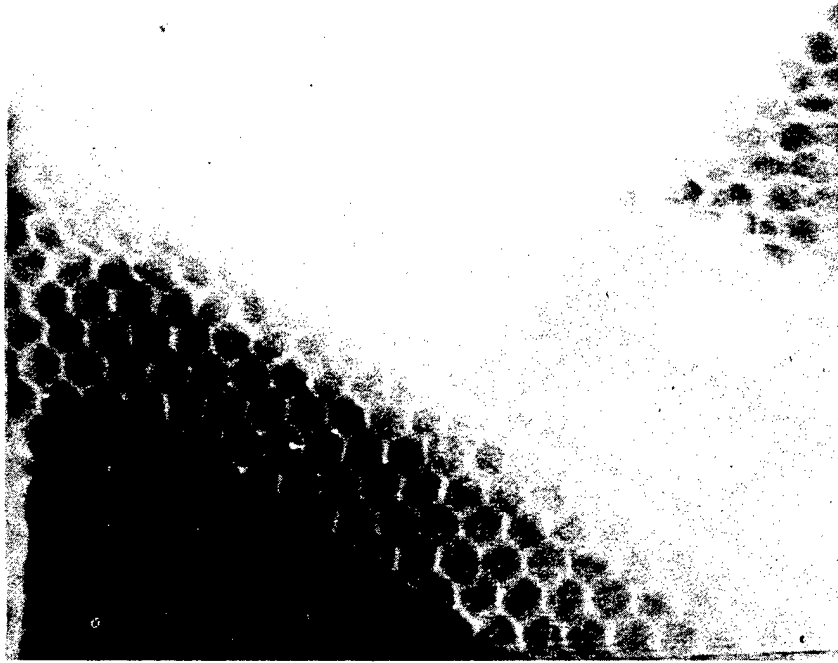


Figure 23. RTR of area H illustrating where the honeycomb is bonded to the aluminum honeycomb. The white areas indicate excessive adhesive (80kV, 4mA)

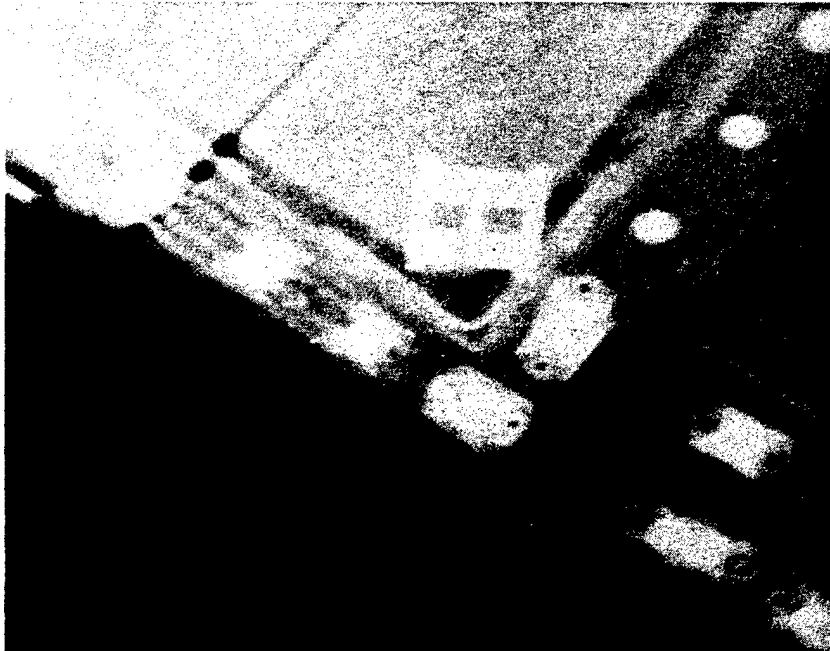


Figure 24. RTR of area H at a higher X-ray energy and current to highlight the metallic area (95kV, 5mA)

in Fig. 23. This illustrates an inherent feature of real-time radiography that allows continuous exposures at increasing x-ray energies to highlight differing materials. This would require multiple film exposures to accomplish the same singular real time inspection.

The second inspection performed at the NARF, Norfolk was on the damaged F-14 radome illustrated in Fig. 25. Figure 26, the RTR of area F, illustrates the damaged honeycomb and cracks (light areas). Also, the porosity or variations in adhesive in the honeycomb occurring during manufacturing are very visible. Another area, B, is shown in the photograph, Fig. 27, illustrates a small nick near the lead label. The RTR, Fig. 28, shows the nick (light area). The same type of porosity indicated in Fig. 26 is seen in this radiograph.

The last example inspected by direct RTR imaging was not for defects or damage, but repair verification. An S-3A spoiler recently repaired by the NARF, Alameda and NADC, Warminster was inspected at SAI to illustrate the feasibility of real-time radiography to image the repaired area and to inspect the splice of the core plug and also the core filter. Fig. 29 shows the repaired area of the graphite/epoxy S-3A spoiler. The RTR, Fig. 30, clearly illustrates the splice, plug, and filler. This radiograph illustrates another feature of the RTR system; the ability to electronically enlarge the image on the videomonitor. This was very advantageous when inspecting the splice and was shown to be superior to film radiographs, because of the ease of viewing the area. Therefore, utilization of RTR for this application would allow inspection to immediately verify the condition of the repair.

In review, the results of using RTR for inspection of composite structures for defects, damage and repair verification indicate that real-time radiography will detect:

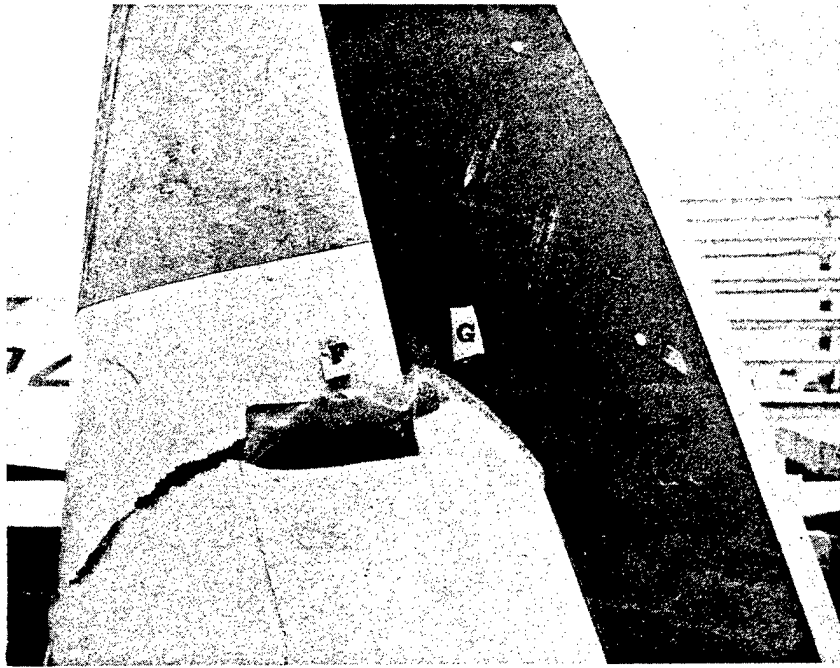


Figure 25. Damaged Fiberglass/Epoxy F-14 Radome containing a fiberglass honeycomb core

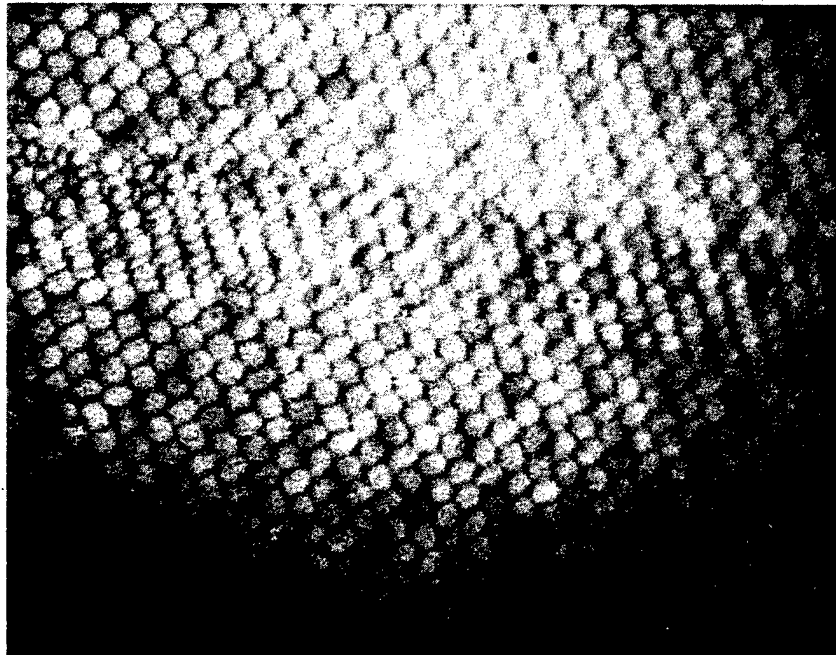


Figure 26. RTR of area F of the F-14 radome illustrating the cracks (white areas) and damaged honeycomb. The variations in the RTR indicate the porosity in the honeycomb. (60kV, 3.6mA)

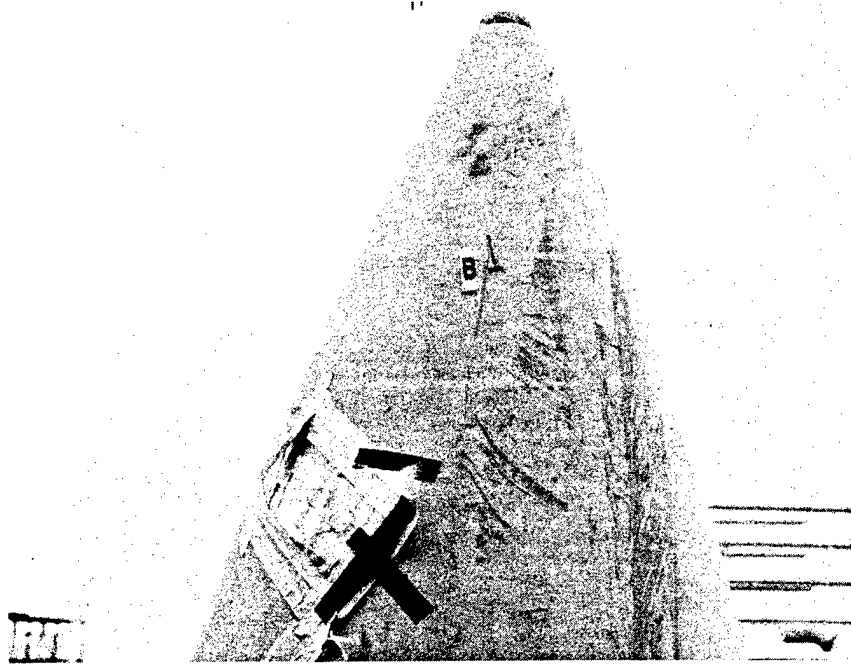


Figure 27. Damaged F-14 radome with a nick visible at area B

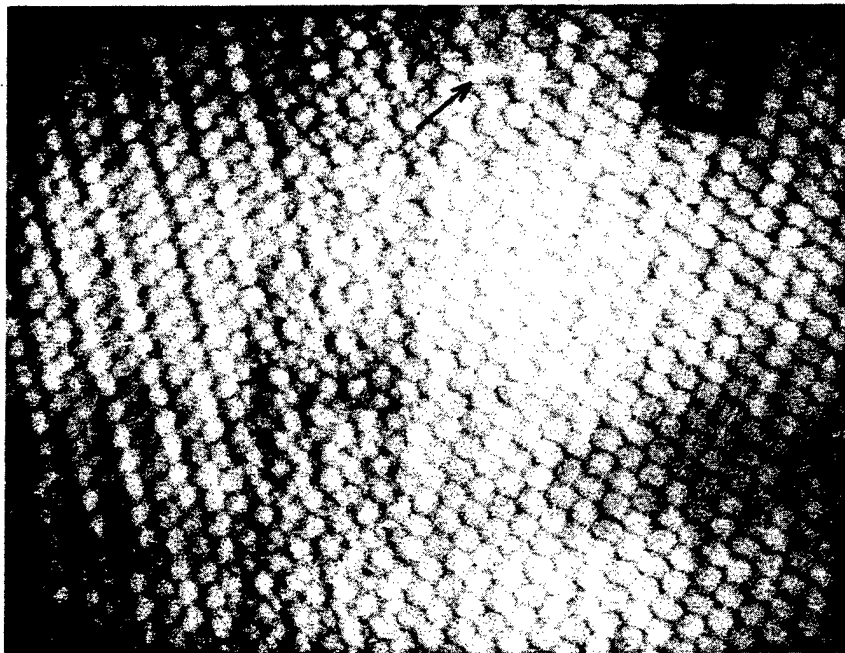


Figure 28. RTR of area B of F-14 radome illustrating the nick (60kV, 3.6mA)

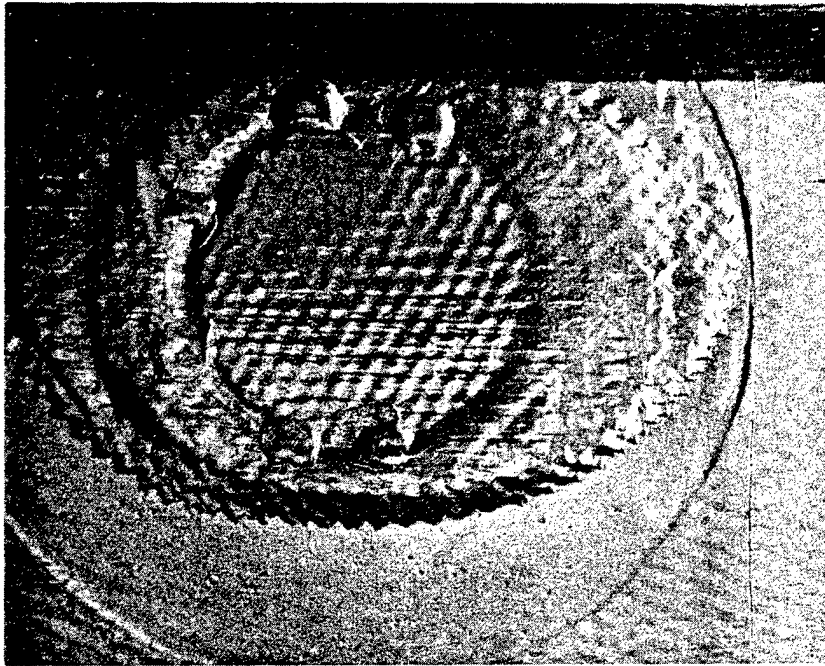


Figure 29. Repaired area of an S-3A graphite/epoxy spoiler

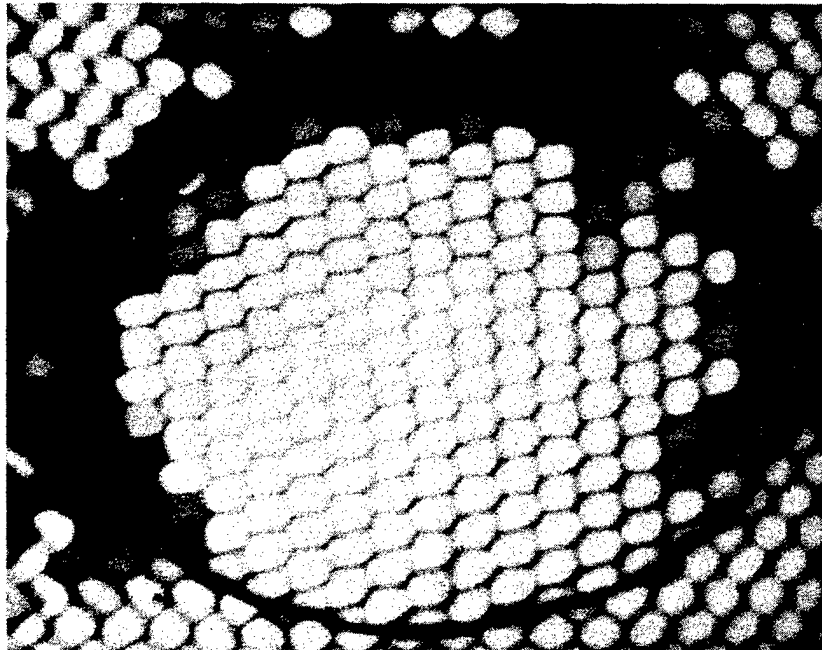


Figure 30. RTR of repaired area illustrating splice and filled core (70kV, 5mA)

- Porosity
- Bondline Voids/Discontinuities
- Moisture Absorption
- Core Damage
- Cracks
- Core splice, plug and filler for repair verification

In addition, the on-site demonstration at the NARF, Norfolk illustrated the advantages of real-time radiography which included:

- Ease of setup for inspecting different structures
- Immediate presentation of the image for defect analysis
- Electronic video enlargement to improve detectability
- Continuous exposure at increasing x-ray energy to highlight both composite and metallic areas in aircraft structures.

#### 4.2 PENETRANT INJECTION RTR INSPECTION

Presently, as discussed in Sec. 2, impact damage areas are inspected visually and with ultrasonics techniques to determine if the area is debonded or delaminated. Then, if the area is debonded, it is cut and patched to prevent further delamination. X-radiography, because of its inability to detect delaminations or debond, is not currently utilized as an NDT technique. However, if an x-ray opaque penetrant could be introduced into the suspect area, the extent of the delaminations/debonds could be determined. Therefore, if an injection system could be developed, x-radiography could be utilized to assess the amount of damage resulting from impact. This section

describes the development of a unique penetrant injection system, that, when coupled with RTR, would greatly facilitate assessment of impact damage to composite structures. Before describing the injection system and results of the RTR inspections, the penetrant selection and RTR detection sensitivity of the penetrant will be discussed.

Various x-ray opaque penetrants, such as TBE, Diiodomethane, lead acetate, and even gases, have been utilized in different laboratory studies to indicate delaminations and debonds. Most of these chemicals, except lead acetate are very dangerous and require special handling. Since this is a study to determine the feasibility of the injection system and RTR imaging, not a study to determine the most effective and non-reacting penetrant, lead acetate was chosen.

A 10% and 20% aqueous lead acetate solution was prepared to determine the sensitivity of the real-time system for these mixtures. Figure 31 is a photograph of a plexiglass test panel that was fabricated with slots of varying depths from .002 inch to .010 inch to measure the absolute RTR sensitivity. Plexiglass was chosen for the test panel because of its similarity to a composite/epoxy structure. These slots were filled with the liquid and the top plate was attached to control the depth and prevent the solution from seeping out. Figure 32 shows an RTR of the 10% solution with the .002 inch depth barely visible. The next RTR, Fig. 33, shows the 20% solution with the .002 inch depth easily seen. Since the total thickness of the test panel was .375 inch, this indicates an RTR thickness sensitivity of less than 1% ( $.002/.375 \times 100\%$ ) for the 20% lead acetate solution. With the penetrant selected and the RTR sensitivity determined, the penetrant injection system will now be discussed.

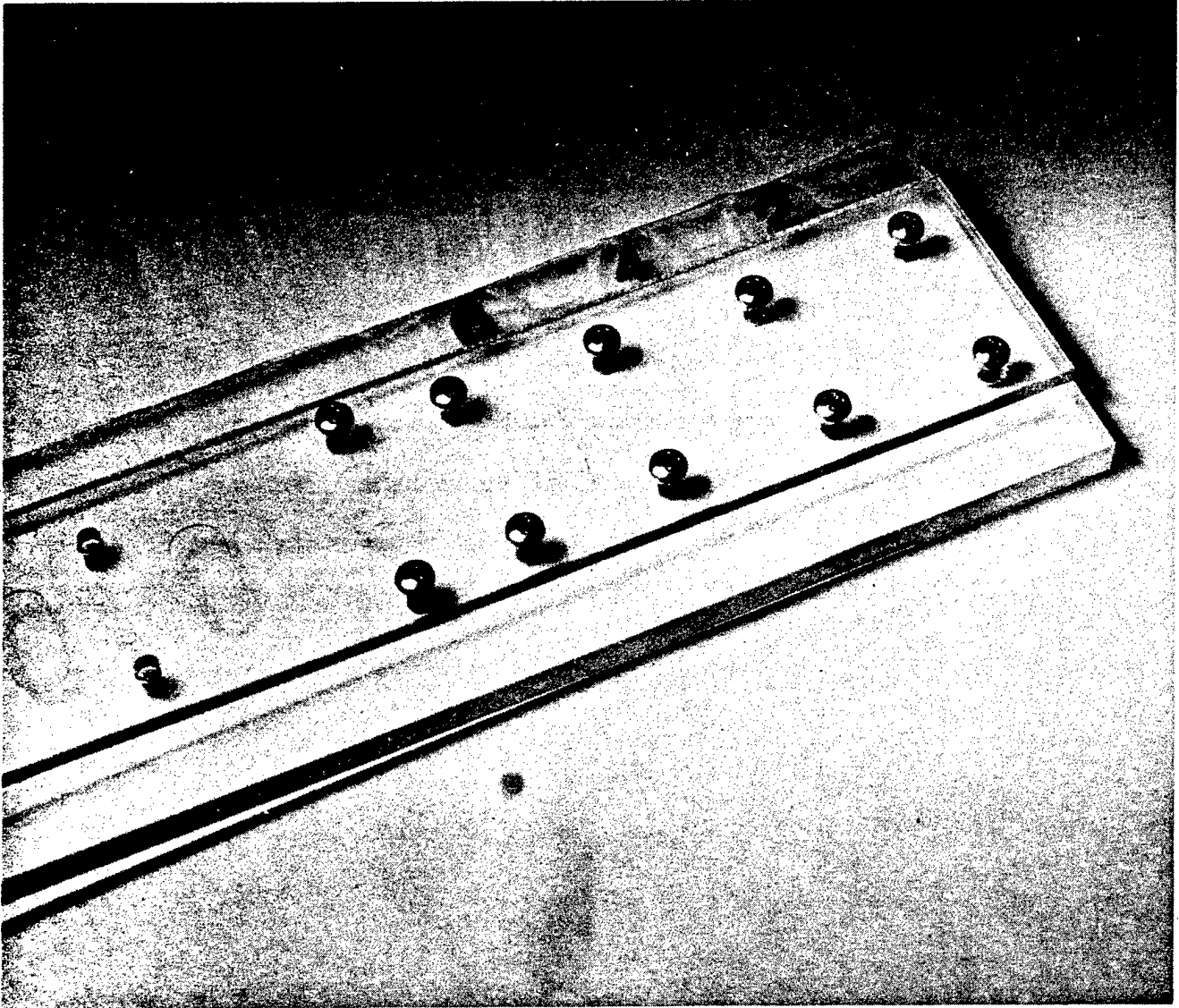


Figure 31. Photograph of plexiglass test panel with slots of varying depths. The lead letters 2, 4, and 6 indicate .002 inch, .004 inch and .006 inch depths.

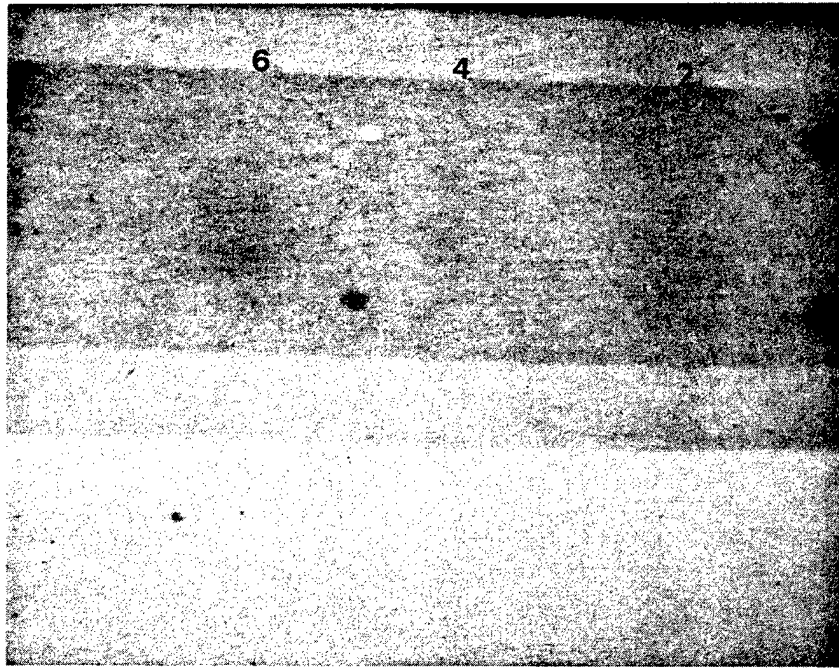


Figure 32. RTR of test panel with a 10% aqueous lead acetate solution illustrating the .002, .004, .006 and .008 inch depths. The .002 inch deep slot is barely visible.

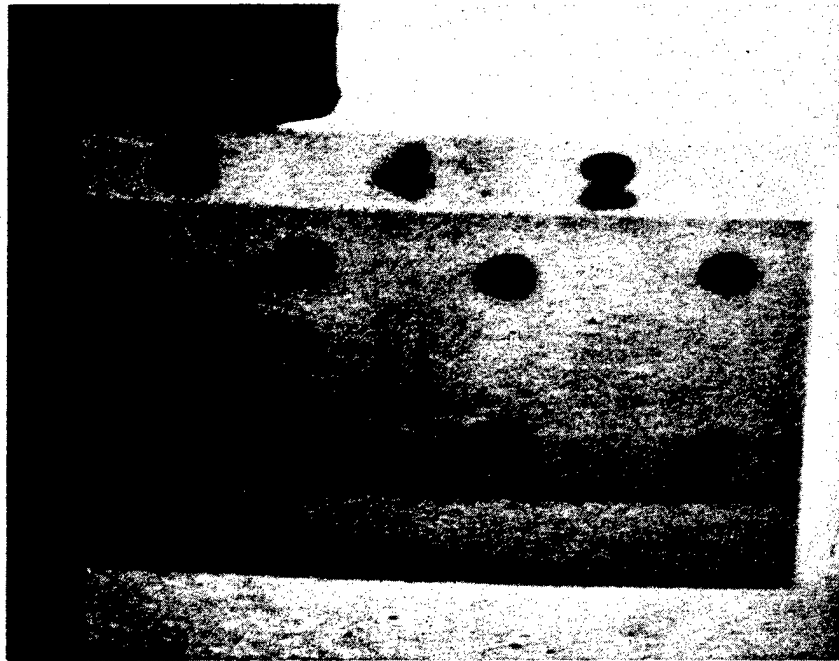


Figure 33. RTR of panel with a 20% lead acetate solution illustrating a significant improvement in resolving the .002 inch deep slot.

Figure 34 shows the prototype penetrant injection system which consists of an air pressure/vacuum pump, pressurized cylinder, and injector tip. The system operates by first filling the cylinder with lead acetate, then pressurizing the liquid to 25 to 30 psi with the air pump. The injector tip is then attached and the system is ready for operation. Injection of the penetrant is accomplished by first drilling a 1/4 inch hole into the area as shown in Fig. 35. The injector tip is then inserted into the hole, as illustrated in Fig. 36, and a 30 inch vacuum is drawn to hold the injector in place. Figure 35 shows the region in the tip where the vacuum is drawn to hold the tip in place. The line to the compressed liquid is then opened, forcing the fluid into the hole. Since the honeycomb is bonded to the skin, the fluid will only flow where there is a debond or delamination.

The first sample tested with the system is shown in Fig. 37. This is a graphite/epoxy sample with aluminum honeycomb that was hit with a hammer to produce debonds and delaminations. A 1/4 inch hole was then drilled and the penetrant was forced into the area. Figure 38, the RTR, shows where the liquid has flowed throughout the area illustrating debonds or delaminations. The next RTR, Fig. 39, shows an electronic video enlargement of the same area, showing areas where the liquid is not in the honeycomb, thus indicating that the liquid has flowed in between the graphite/epoxy layers.

Another sample, a piece of an F-14 boron/epoxy horizontal stabilizer, Fig. 40 was hit with a hammer and injected with the penetrant to determine the extent of the damage. Figure 41 is an RTR of the area showing that there is no apparent physical damage to the structure. The light area in the radiograph is the 1/4 inch drilled hole. Figure 42, the RTR of the area with the penetrant, illustrates that the liquid has flowed throughout a much larger area than indicated by

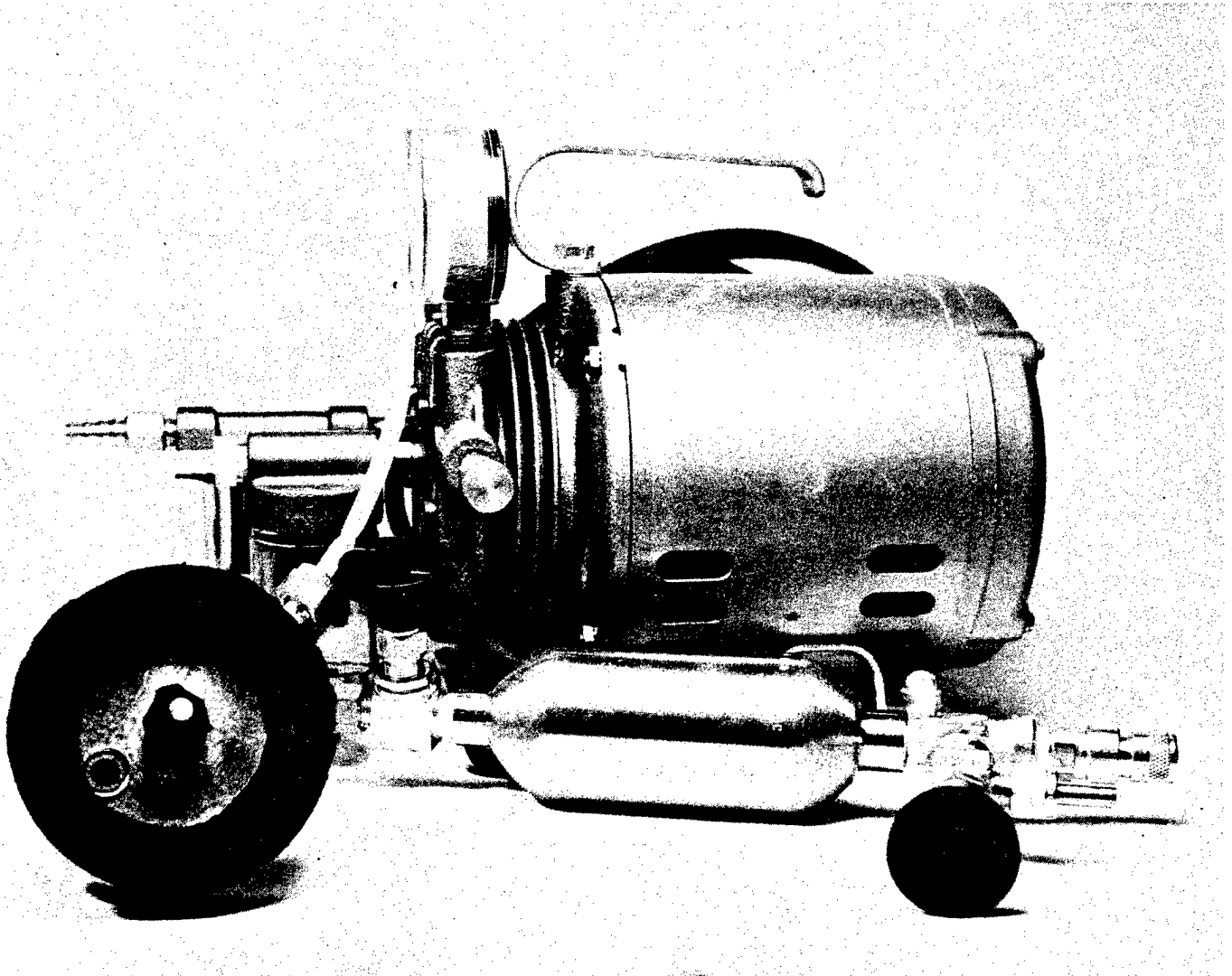


Figure 34. Penetrant injection system consisting of air pressure/vacuum pump, pressurized cylinder, and injector tip.

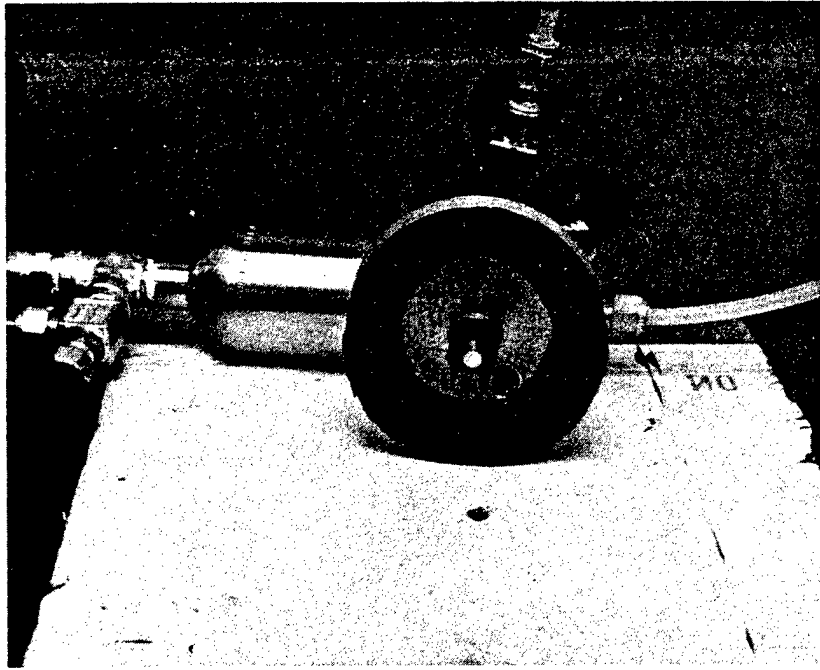


Figure 35. Photograph of the injector tip before insertion into the 1/4 inch drilled hole in a F-14 Boron/Epoxy horizontal stabilizer sample

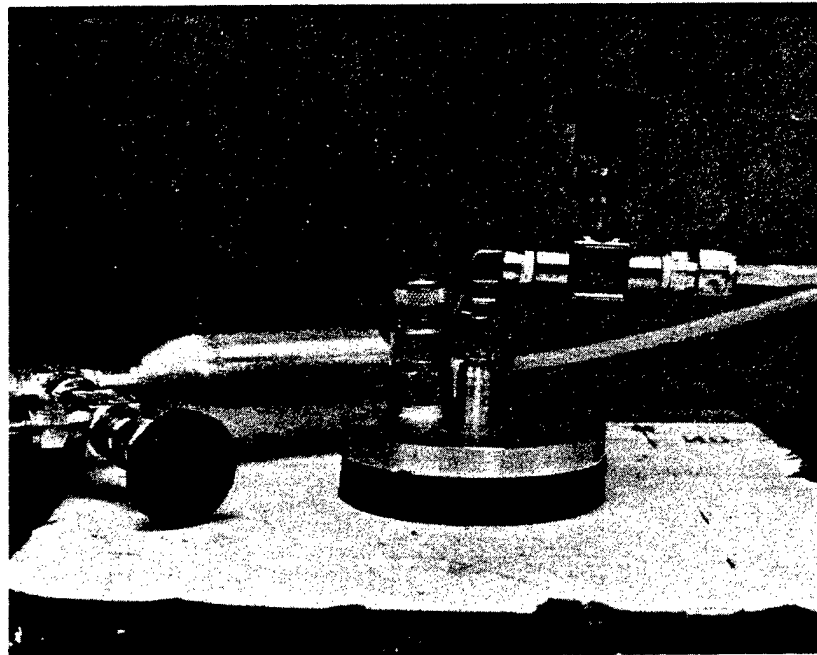


Figure 36. Photograph illustrating the operation of the injection system

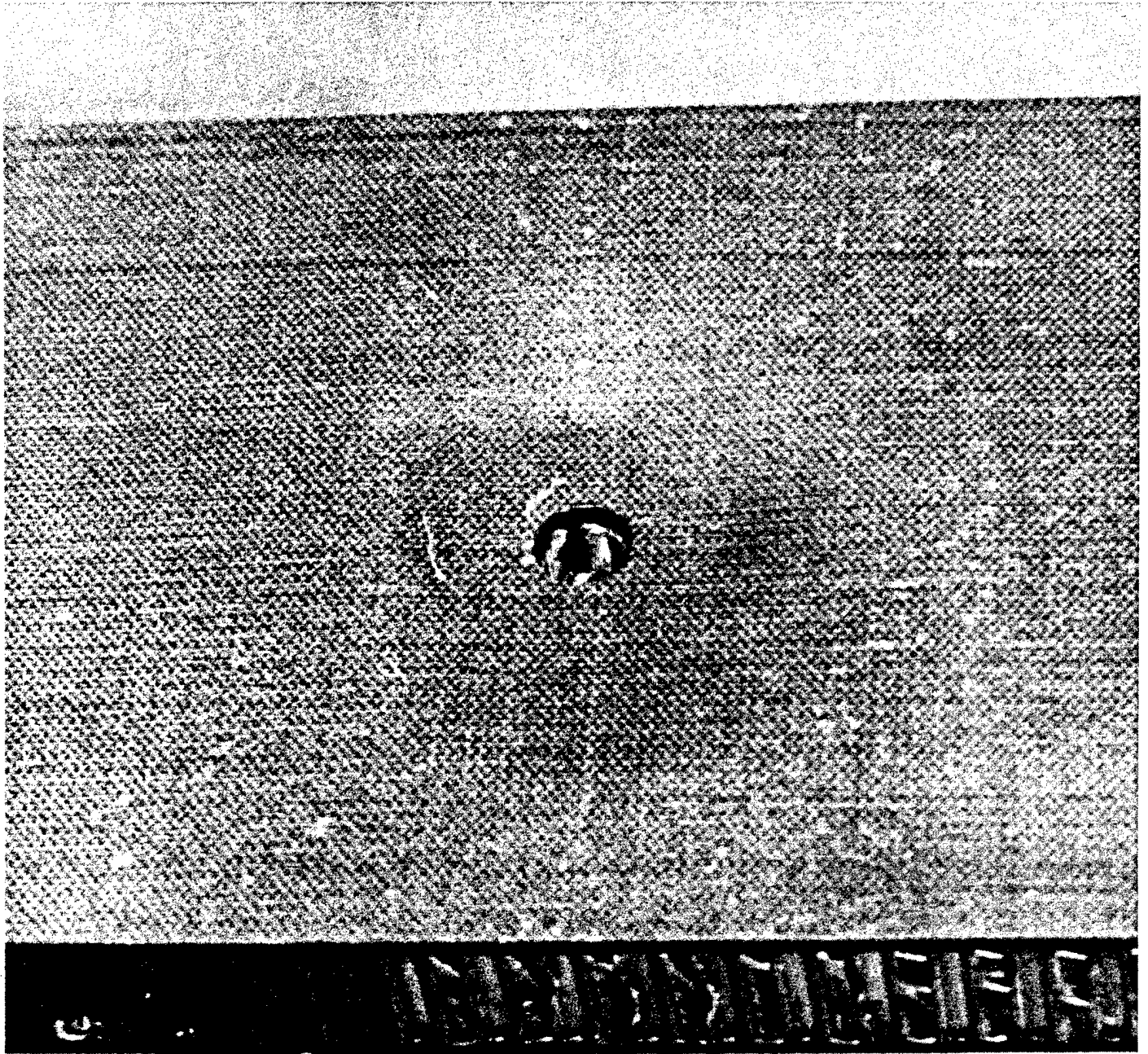


Figure 37. Photograph of a section of a Graphite/Epoxy sample with aluminum honeycomb. It has been damaged by hitting the area with a hammer. A  $\frac{1}{4}$  inch hole has been drilled for the injector tip.

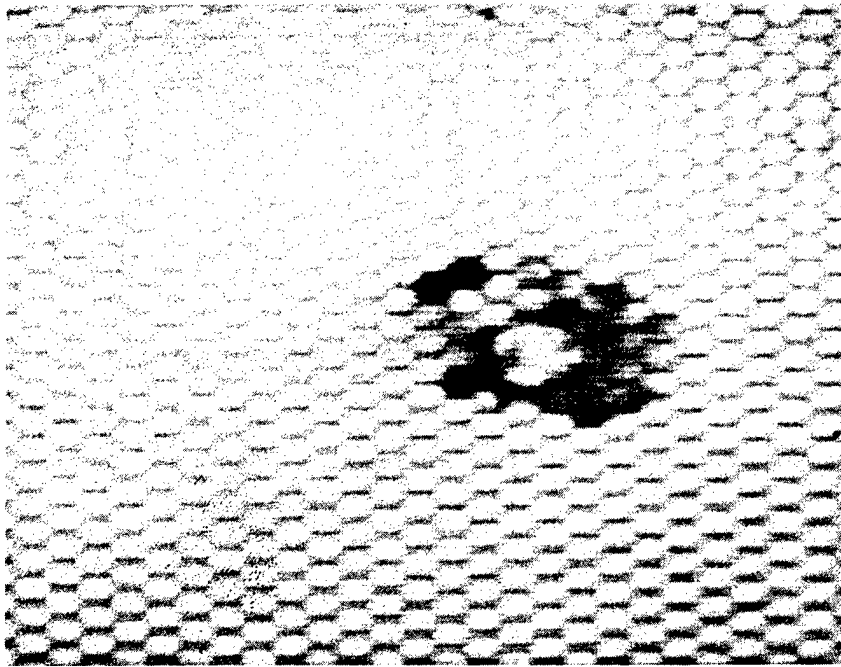


Figure 38. RTR of the damaged area illustrating where the penetrant has flowed into the honeycomb and possibly between the laminations indicating debonds and delaminations (65kV, 5mA)

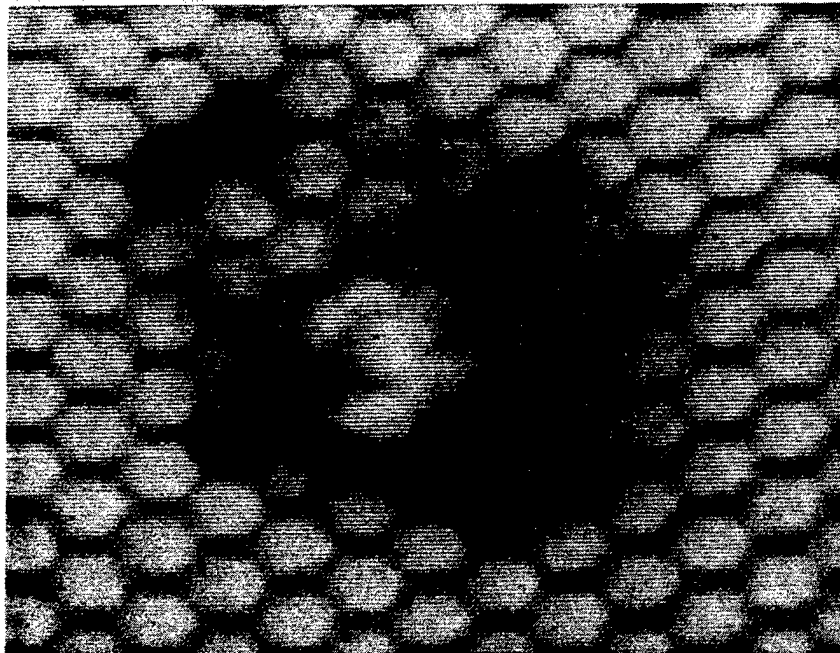


Figure 39. Electronically enlarged RTR, Figure 37, illustrating an improvement in detectability. This is a standard feature of the RTR-100 system.

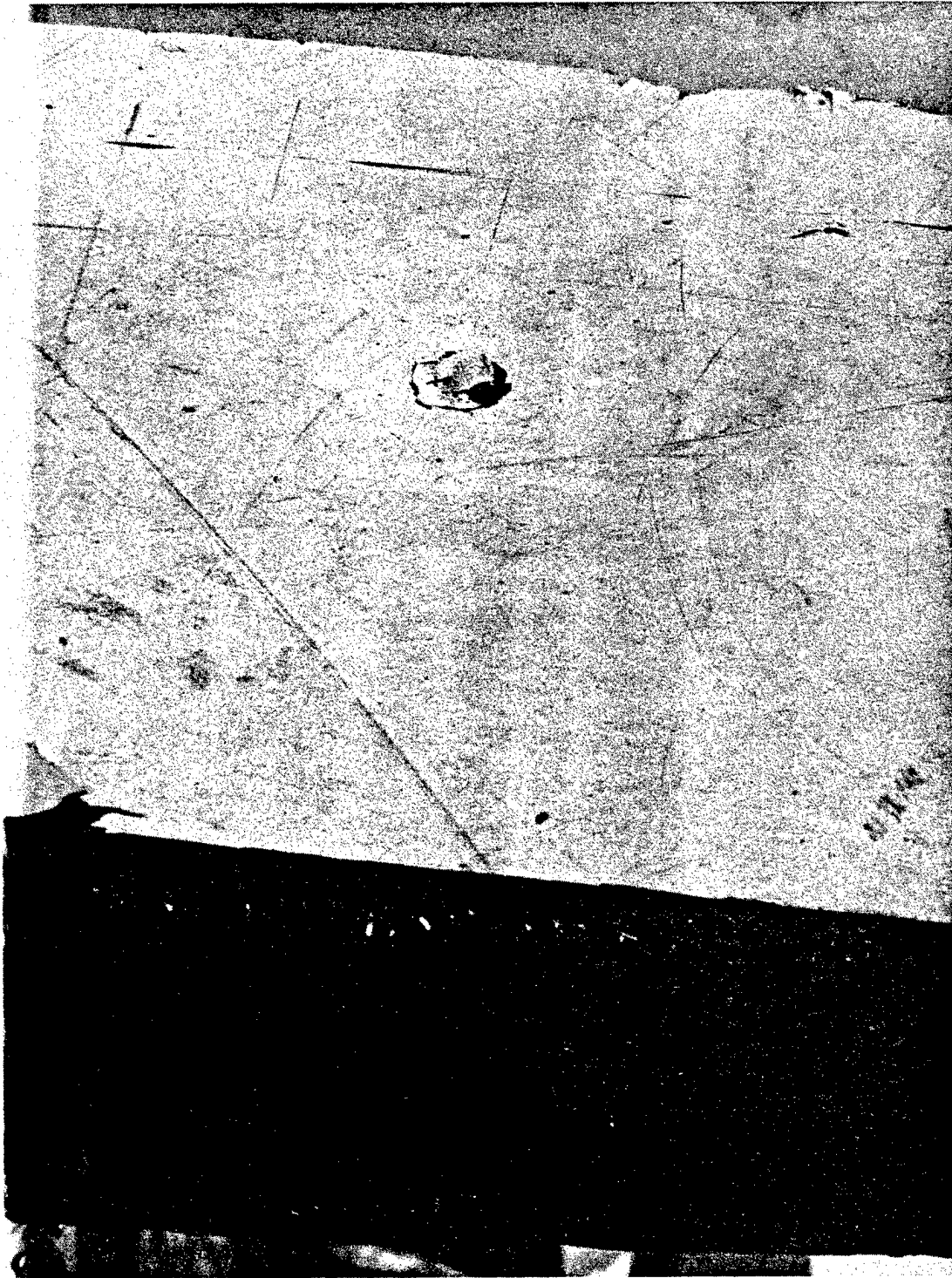


Figure 40. Photograph of a small damaged area with a  $\frac{1}{4}$  inch drilled hole for the injector tip. This is a F-14 Boron/Epoxy horizontal stabilizer section.

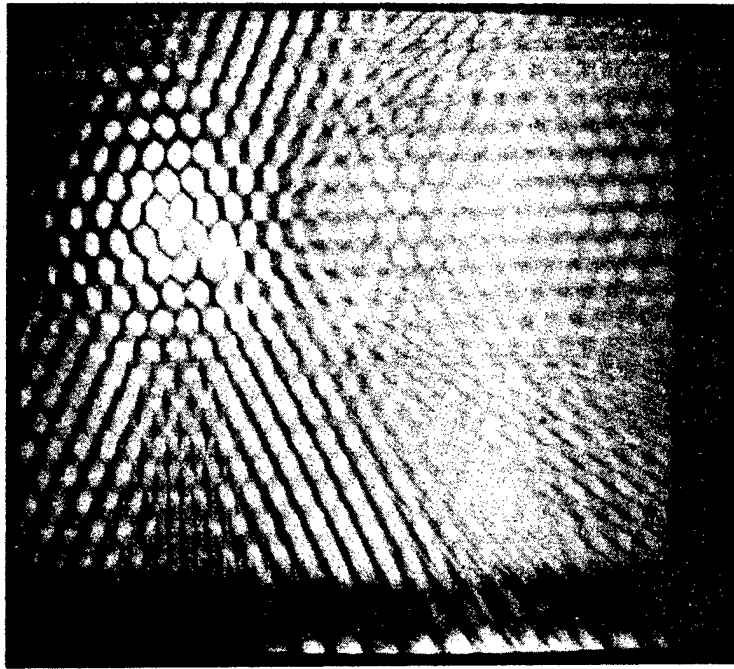


Figure 41. RTR of the damaged section, with no visible indication of damage. The light area is the  $\frac{1}{4}$  inch drilled hole (65kV, 5mA)

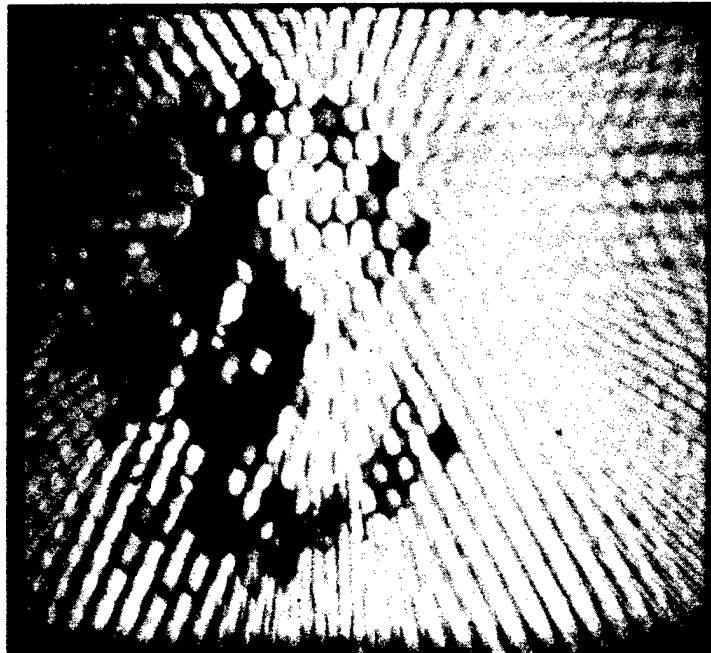


Figure 42. RTR of damaged area illustrating where the penetrant has flowed throughout the piece. This indicates fairly excessive damage for relatively small surface damage (65kV, 5mA)

the surface damage. The radiograph shows that the penetrant has filled many honeycomb cores, indicating debonds; but it is very difficult to determine if there are any delaminations between the boron/epoxy layers.

In order to determine if the liquid would flow into delaminated areas, a 6-ply graphite epoxy sample without any honeycomb was tested. Figure 43 shows the graphite/epoxy sample damaged to varying degrees with a hammer. A 1/4 inch hole was drilled into the areas as before and the injector was inserted. Since there was no honeycomb to seal the tip for the penetrant flow, a small box was made for the bottom. This created a seal which would allow the penetrant to flow into the delaminated layers. Figure 44 shows the RTR of the piece illustrating that the liquid has flowed into the delaminated layers. The differences in contrast indicate areas containing varying amounts of penetrant, thus indicating varying amounts of delamination. Figure 45 shows another area that contains a large amount of penetrant throughout, indicating a substantial amount of delaminations. The corner of the piece was visually delaminated in three or four layers and during the tests was completely filled with the penetrant.

These preliminary results show the feasibility of a penetrant injection system that, when coupled with RTR, would detect delaminations and debonds in test pieces with a relative thickness sensitivity of about 1%.

These successful results suggest that further work should be performed to design and fabricate a portable penetrant injection system that could be utilized to assess the amount of damage resulting from impact. This work should include development of an effective injector tip, with parameters such as penetrant type, penetrant pressure, liquid penetrability and delamination sensitivity investigated to produce an optimum technique.



Figure 43. Photograph of a six-ply graphite skin with varying amounts of damage

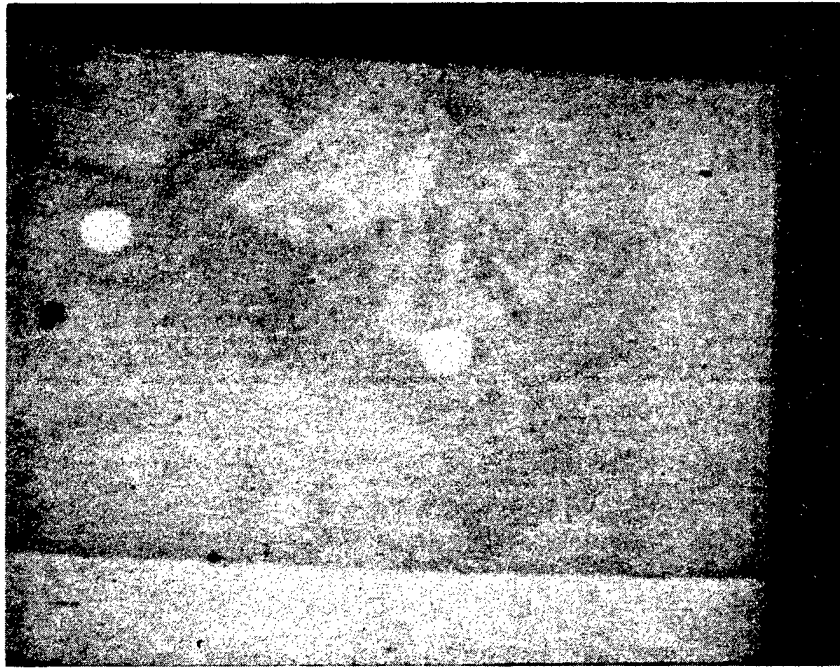


Figure 44. RTR of areas illustrating where the liquid has flowed into the delaminations (65kV, 5mA)

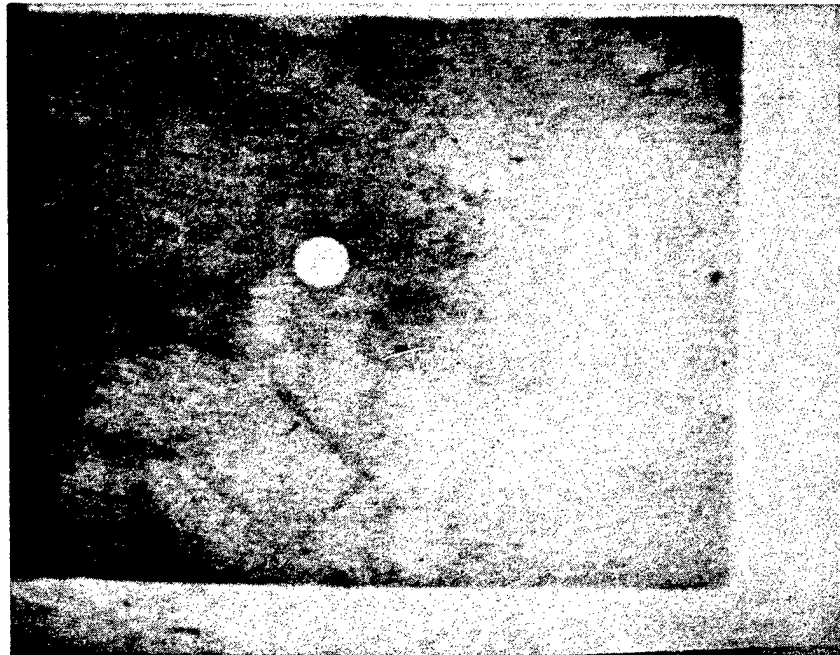


Figure 45. RTR illustrating excessive delaminations throughout the area, indicated by the large amount of the penetrant in the area (65kV, 5mA)

## 5. SUMMARY, CONCLUSIONS AND RECOMMENDATIONS

### 5.1 SUMMARY OF RESULTS

The results of utilizing direct RTR inspection of composite structures consisting of:

- Fiberglass/epoxy laboratory samples
- Graphite/epoxy laboratory samples
- F-14 boron/epoxy horizontal stabilizer
- F-14 fiberglass/epoxy radome
- S-3A graphite/epoxy spoiler

indicate that RTR could be utilized to detect:

- Porosity
- Bondline voids/discontinuities
- Moisture absorption
- Core damage
- Cracks
- Core splice, plug and filler for repair verification.

In addition, the on-site demonstration at the NARF, Norfolk, further illustrated the feasibility of utilizing RTR at the depot level. This demonstration indicated the inherent features of RTR for composite inspection which included:

- Ease of set up for inspecting different composite structures
- Immediate presentation of the image for defect analysis

- Electronic video enlargement to improve detectability
- Continuous inspection at increasing x-ray energy to highlight both composite and metallic areas in an aircraft structure.

For the penetrant injection inspections, with a 20% aqueous lead acetate solution, the results indicate that RTR will detect:

- 2 mils of the solution in test panel
- The extent of debonds and delaminations in graphite/epoxy and boron/epoxy lab samples

## 5.2 CONCLUSIONS

Real-Time Radiography can be utilized to adequately detect composite defects and damage as well as aid in the verification of repairs.

Real-Time Radiography can be effectively utilized at the depot level to complement or replace film exposures for composite structural inspections. This technique would:

- Greatly reduce inspection time.
- Greatly reduce costs associated with film and film processing
- Increase the inspection capability at the depot level.

The prototype injection system coupled with RTR illustrated the feasibility of the technique for assessment of impact damage for debonds and delaminations.

## 5.3 RECOMMENDATIONS

- Implement Real-Time Radiography to complement or replace present techniques for composite aircraft inspection

- Procure RTR systems, fabricated to meet the Navy's requirements, for maintenance levels
- Initiate a program to develop a portable penetrant injection system that could be utilized at the 1 and 0 levels for assessment of impact damage for delaminations and debonds. This program would consist of:
  - Determining penetrant type, penetrant effect on composites, and sensitivity of RTR to penetrant
  - Determining the design and operational parameters for optimum penetration and sensitivity
  - Determine the debond and delamination sensitivity

In addition, after these parameters were determined, the system could be tested at selected NARF's and organizational levels to demonstrate the effectiveness of the technique.

## REFERENCES

1. Demonstration of SAI Real-Time Radiography System for Naval Aircraft X-Ray Inspection, SAI-78-528-LJ, February 6, 1978, F. Patricelli, R. Polichar, V. J. Orphan. \*
2. Composite Material Maintenance/Repair Workshop sponsored by the Naval Air Systems Command held at San Diego in September, 1978, S-3 Graphite Spoiler Repair, Ed Rosenzweig, Naval Air Development Center, p. 112. \*
3. ibid, F-14 Boron Epoxy Horizontal Stabilizer Repair, Jim Candela, NESO, Norfolk, p. 136.
4. ibid, CH-46 Hybrid Composite Rotor Blade, T. Hammer and N. Dicroce, Boeing Vertol, p. 173.
5. ibid, Repair of DC-10 Stabilizer, E. Slaven, Douglas Aircraft, p. 127.
6. ibid, Survey of NDI Capability within the DoD Community, Sharon McGovern, Vought Corp., p. 206.
7. ibid, Survey of NDI Capability Within the DoD Community, Sharon McGovern, Vought Corp., p. 208.
8. ibid, F-14 Boron Epoxy Horizontal Stabilizer Repair, Jim Candela, NESO, Norfolk, p. 139.
9. ibid, F-14 Boron Epoxy Horizontal Stabilizer Repair, Jim Candela, NESO, Norfolk, p. 140.
10. ibid, F-14 Boron Epoxy Horizontal Stabilizer Repair, Jim Candela, NESO, Norfolk, p. 141.
11. ibid, S-3 Graphite Spoiler Repair, Ed Rosenzweig, Naval Air Development Center, p. 114.
12. ibid, S-3 Graphite Spoiler Repair, Ed Rosenzweig, Naval Air Development Center, p. 116.
13. ibid, Survey of NDI Capability Within the DoD Community, Sharon McGovern, Vought Corp., p. 207.
14. Utilization of Real-Time X-Radiography for In-Service Inspection of Nuclear Reactor Piping: Feasibility Investigation, EPRI NP-950, Project RP607-2, December 1978, by F. Patricelli, J. Baltgalvis, R. Polichar, V. Orphan.

\* NAVAIRSYSCOM (AIR-4114C) reports, demonstrations, and maintenance application under the Maintenance Technology Program

NADC-77073-30

U. S. Army Aviation Systems Command (CCAD/SAVAE-GG) . . . . . 1  
Corpus Christi, TX 78419

U. S. Army Materials & Mechanics Research Center. . . . . 1  
Watertown, MA 02172

U. S. Army Air Mobility Research & Development Lab. . . . . 1  
AMES Research Center, Moffett Field, CA 94035

Chief Petty Officer in Charge . . . . . 1  
Service School Command Glakes  
Detachment Chanute, TWSMN  
Chanute AFB, IL 61868

DDC . . . . . 12

LIBRARY (8131). . . . . 3

U 810 0141  
Science Applications, Inc.

NADC-77073-30

DATE	ISSUED TO

**NAVAL GENERAL LIBRARIES**  
**(CHIEF OF NAVAL TRAINING SUPPORT)**

D I S T R I B U T I O N   L I S T

No. of Copies

NAVAIRSYSCOM (AIR 954) . . . . .	5
2 for retention	
1 for AIR-4114C	
1 for AIR-5203	
1 for AIR-320	
NAVMAT (Code 08EB) . . . . .	1
ONR (Code 211) . . . . .	1
NRL (Code 6170) . . . . .	1
COMNAVAIRLANT (Code 528) . . . . .	1
COMNAVAIRPAC (Code 74) . . . . .	1
NAVAIREWORKFAC, NAS, Alameda (Code 300 & 340) . . . . .	2
Jacksonville (Code 300 & 340) . . . . .	2
North Island (Code 300 & 340) . . . . .	2
Norfolk (Code 300 & 340) . . . . .	2
Pensacola (Code 300 & 340) . . . . .	2
MCAS, Cherry Point (Code 300 & 340) . . . . .	2
COM NAR (Code 32) . . . . .	1
CNATRA . . . . .	1
NAVAIRENGCEN (ESSD ES-1) . . . . .	1
(GSED Code 92713) . . . . .	1
NAVAIRTESTCEN . . . . .	1
NAVMIRO (Code 224) . . . . .	1
CMC (Code AA J5) . . . . .	1
San Antonio Air Materiel Area (MMEW) . . . . .	1
Kelly Air Force Base, TX 78241	
Air Force Materials Laboratory (AFML/LTM) . . . . .	1
Wright Patterson AFB, OH 45433	
Sacramento Air Logistics Center (MAGC) . . . . .	1
McClellan AFB, Sacramento, CA 95652	
Warner-Robins Air Materiel Area (MME) . . . . .	1
Robins AFB, GA 31094	

8100141

CONTINUED ON INSIDE OF COVER